POLITECNICO DI TORINO

MASTER's Degree in Mechatronic Engineering

Politecnico
di Torino

MASTER's Degree Thesis

Analysis, modelling and design of a multi-joint under-actuated leg prosthesis based on EHA

Supervisors

Prof. ANDREA TONOLI

Prof. NICOLA AMATI

Ph.D. FEDERICO TESSARI

Eng. MARCO PULITI

Prof. RENATO GALLUZZI

Candidate

Michele PARAVANO

DECEMBER 2022

Abstract

Leg prostheses in the market and in literature that actuate both knee and ankle joint are usually heavy and discarded by the patients for lighter semi-active ones. The purpose of this thesis is to study the possibility to realize a multi-joint under-actuated leg prosthesis based on Electro-Hydrostatic Actuation (EHA), as to have only one power unit for both joints, reducing the bulkiness and overall weight. Hydraulics motion transmission can serve an optimum role in such application, as power transfer between the components is an easier task as the motor does not have to be placed close to the actuated joint. The hydraulic circuit actuating the prosthesis is made up of an EHA unit composed of a fixed-displacement pump and an electric synchronous motor; two hydraulics actuators (double-acting hydraulic cylinders) are connected to the EHA and are in direct configuration (upper chamber connected to upper chamber). Finally, a bi-directional valve is linked in series to the upper chamber of each cylinder to allow for stroke modulation.

The theoretical analysis of the available physiological dataset and the dimensioning of the components was performed in MATLAB® environment, while simulation and control of the prosthesis was carried out in Simulink® via Simscape™ and Multibody modelling tools.

The simulation allowed us to confirm the theoretical results and to verify that the prosthesis works with the predefined components and follows the physiological trajectories with a low RMSE in a open loop control. Moreover, this prosthesis, by under-actuated design, has the advantage of being able to power both joints with one motor and decouple joint movement for different tasks thanks to the implemented valves. These design traits make such prosthesis possibly able to actuate both knee and ankle for different ambulatory tasks while maintaining a lighter weight with respect to its fully-active counterparts.

Summary

This thesis' objective is to inquire in the possibility of developing a light-weight semi-active multi-joint prosthesis for transfemoral amputees that can supply the patient's needs of stable assistance during the gait, while reducing the weight and bulkiness with respect to the fully active knee-ankle prostheses currently in research or on the market.
Under-actuation and semi-active hydraulic actuation are the principal characteristic of this prosthesis, motivated by the adaptability of hydraulic transmission in such high power/volume ratio application.
The prosthesis in study consists of a support structure (chassis) and an actuation circuit. The latter is one of the main topics of research of this thesis. The hydraulic circuit power unit is a motor-pump system, made up of an Electro Hydrostatic Actuation (EHA) unit which consists of a fixed-displacement pump and a synchronous electric motor. This is then connected to two double-acting hydraulic actuators (cylinders) by means of hydraulic delivery lines linked in a direct configuration (upper chamber of one cylinder connected to upper chamber of second hydraulic cylinder). A variable arm linkage allows to transform the linear motion of the cylinder into the rotary one of the joints. In fact, the cylinders are positioned respectively behind each joint. To modulate the movements of the cylinders, two hydraulic valves are implemented. The partial shutting of one or both valves allows to actuate the leg accordingly to the physiological walking trajectory. Moreover, by shutting completely one of the two valves, the joints can be decoupled and one degree of freedom is completely blocked, which can be a useful trait when having to deal with complex movements such as stair ascending and even walking. To determine the dimensions of the various components of the prosthesis, a theoretical analysis of a dataset containing physiological gait data was carried out: data from 50 subjects was taken from an existing dataset and averaged. The most relevant part of this dataset of physiological aspects were angles, forces and torques of hip, knee and ankle joints. Thanks to this averaged data, it was possible to carry on with a design of the prosthesis that could fit the average subject.
One important aspect for the prosthesis, was to optimize the cylinders attachments positioning on the leg. This was done by minimizing the lever arm of the knee

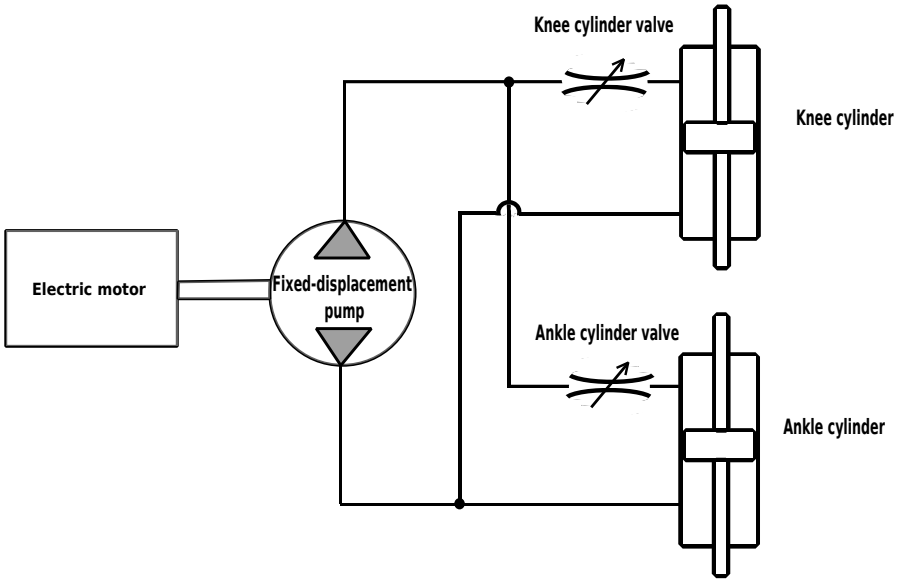

Figure 1: Hydraulic circuit schematic

joint (to have a knee with high backdrivability) and by maximizing the lever arm of the ankle joint (so that the forces on the ankle cylinder could be minimized). It is important to note that the reason for this can be retrieved in the need of the knee joint to reach high velocities, while for the ankle joint to exert high forces. In addition, it was pointed out that, since the gait cycle (walking cycle) is characterized by two main phases, the "Stance phase", which exhibits high forces, and, the "Swing phase", which is characterized by high velocities, it would be better to actively power the joints during the "Swing phase", and only partially assist during the "Stance phase". Such choice is motivated by preliminary studies which show that a partial assistance during high torque requiring phases is perceived as a good deal of help by patients. In contrast, assisting the "Stance phase" fully, would result in bulky and heavy actuators due to higher torque requirements, which would impede the ergonomics, weight and comfort of the prosthesis. Last but not least, valve modulation can play an important role in modulating the prosthesis movement passively: the controlled action of motor plus valves could then result in a prosthesis with a good movement versatility and a good degree of assistance for activities of daily living. Thanks to this theoretical analysis, which was carried out in the MATLAB® environment, useful data was extrapolated, such as velocities and accelerations of the joints and cylinders. Consequently, flows and forces could be retrieved, which led to the "Swing-oriented design" of pump and electric motor. Such theoretical results were then confirmed via simulation in the Simulink® Simscape™ environment, where, firstly, all the circuit components were tested to verify their functioning, and, secondly, the hydraulic circuit was put together

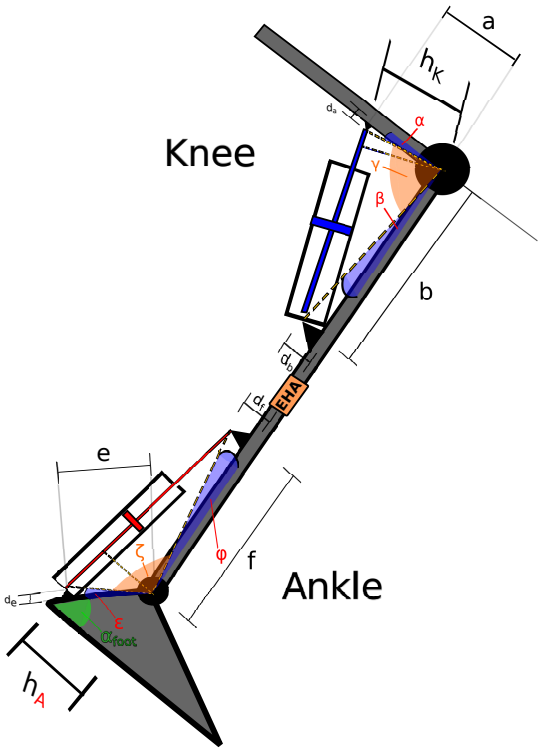

Figure 2: Prosthesis schematic with parameters

to confirm the pump and motor capabilities of actuating the leg. This was done thanks to an open-loop control simulation, where a custom reference was created for the motor torque. It was confirmed that the chosen motor torque and pump displacement could indeed provide sufficient actuation of the leg during the swing phase.
In addition, hip movement was added to the simulation. The latter relaxed by a good amount the effort that the motor has to undergo during the swing, since, in a normal gait, the hip movement has a major effect in helping the leg swinging forward. In fact, the hip transfers its inertial contribution to the lower leg, propelling it forward. The results of the simulation were satisfactory in the sense that the knee and ankle joints followed closely their physiological trajectory. Moreover, the motor always worked under its rated torque line thanks to the hip movement assistance, so we are in a good condition to prevent losses due to heat.
The theoretical analysis and simulation showed that such prosthesis can be realized and that its overall weight and power are are inside the predefined bounds for a lightweight prosthesis, which was ultimately the objective of the thesis. Lastly, thanks to the EHA unit, energy-regeneration principles can be applied since the "Swing phase" of the gait cycle offers windows of opportunity for such application.

Acknowledgements

To my family, who made all of this possible. I hope to learn to love how you loved me. To the teachers in my life, who led me through my path, in particular, to Marco and Federico for the formidable support and knowledge they gave me during my thesis. To my girlfriend Santa, who is my inseparable companion of life. To the Camplus and IIT center and community, which allowed me to have an eye opening learning experience. Lastly, to Politecnico di Torino, which through hardships and joys, brought me here.

Table of Contents

List of Tables

List of Figures

Chapter 1

Background

Introduction Individuals who undergo an amputation during their life may use a prosthetic leg. There are many types and can be divided in different subcategories, mainly differentiated by the type and place of the amputation and the assistance that they give.
The prosthesis has to help the individual in the primary locomotor task: walking. The walking phases are described by the **gait cycle**.

Figure 1.1: Evolution of leg prostheses [1]

1.1 The anatomy of walking: Gait Cycle

The gait cycle is the action of walking repeating itself, as such, it is a cycle. It is divided in two main phases: the stance phase and the swing phase. The gait cycle conventionally starts when the heel touches the ground for the first time and ends when the cycle completes, so when the heel touches again the ground after having completed a step. These two main phases are themselves divided in sub-phases with specific terms to indicate the action performed during said phase:

- **Stance phase**:
  - *Heel strike (0% gait cycle)*: The heel touches the ground so now both legs are supporting the weight, which starts to shift and increase on the leg that just landed.
  - *Foot flat (8-10% gait cycle)*: The foot continues to absorb the weight while the knee brakes its flexion and supports the body.
  - *Mid-stance (20-25% gait cycle)*: The opposite leg is lifted, leaving the body in balance. In this phase the knee torque is highest, while the ankle keeps dorsiflexing and loading the Achilles tendon as a spring.
  - *Heel off (40-45% gait cycle)*: The heel raises from the ground and the weight shifts on the front of the foot, this is the moment where the ankle produces the biggest torque. The foot plantarflexes.
- **Swing phase**:
  - *Pre-swing (50-60% gait cycle)*: The whole foot starts to lift from the ground due to the combined action of hip movement and knee flexion.
  - *Swing (60-85% gait cycle)*: The knee first ends its flexion, raising up the leg, following this, it extends to swing the leg forward and carry the foot in the initial position of the next gait cycle. During this phase, the foot dorsiflexes to go in the "toe clearance" position, so that it doesn't hit the ground during the swing.
  - *Late-swing, deceleration (85-100% gait cycle)*: The knee decelerates and carries the foot in the "Heel strike" position. The cycle ends.

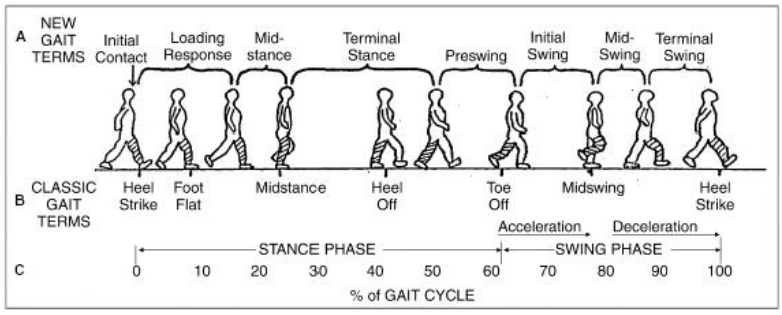

Figure 1.2: Gait Cycle and corresponding phases [2]

1.2 Types of prostheses

Depending on the level and dimension of the amputation, different solutions can arise, here we will take into account only partial or full leg amputations, as the scope of this thesis is a transfemoral prosthesis:

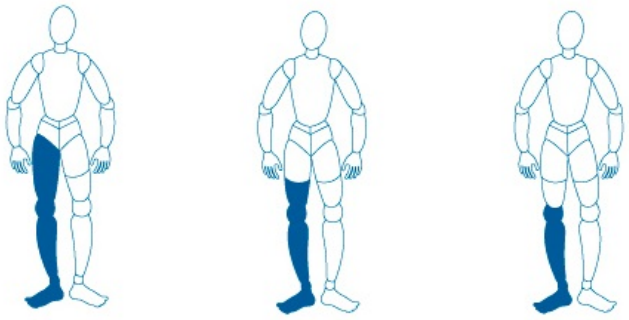

Figure 1.3: Amputation levels for a transfemoral prosthesis [3]

In the transfemoral case, as for all prosthesis, we can distinguish between *passive*, *active* and *semi-active* prostheses.
In addition, active prostheses differ in the type of actuation. Different type of actuation have respective advantages in terms of power, volume and comfort with respect to other solutions, as pointed out by Windrich et al. in [4]. More specifically, leg prostheses have primarily a structural support function as during walking and locomotory tasks they have to hold effectively the whole body weight. Secondarily, they could provide an aid to joint motion.

1.2.1 Passive prostheses

These type of prostheses have no active power inputted in the prosthesis itself: they can although replicate the structural function of the leg and a sufficient joint motion for standard tasks. They rely on the movement of the hip and body for propulsion of the limb.
These type of prostheses are preferred by athletes who want to run or jump, as these tasks imply high velocities and forces which could be very difficult to be exerted by an active prostheses with motors, so an elastic type of aid is preferred. Indeed elastic feet are the primary mean of propulsion for such tasks. Moreover, it is much more simple to learn how to use and walk with a passive prosthetic leg, as it is a simpler object. These types of prosthetic legs are the simplest kind and the first ones to appear historically.

1.2.2 Active prostheses

After passive prosthesis, come active prosthesis, which, with active power, actuate the limb during *all* the phases of the gait cycle. In fact, powered knee-ankle prostheses are capable of providing net-positive mechanical energy to amputees. To realize these objectives, they require large amounts of power, which usually result in bulky actuators and prostheses in general, as developing an active prosthesis that reaches the actuation performance of the lost limb, is a challenge in and of itself, especially if we want to remain under the original limb weight [5]

1.2.3 Semi-active prostheses

The newest generation of prostheses usually resides in this category. Semi-active prostheses actuate the knee and/or ankle joints only in certain phases of the gait, as high torque braking phases can be carried out thanks to the use of adaptive dampers. This kind of actuation allows to decrease the overall weight and volume of the prosthesis, while having less power consumption. These prostheses require a good high and low level control to properly understand when to use the motors to actuate the joints and when to stop them.
The prosthesis in discussion in this thesis also falls under this category.

1.3 Another characterization for transfemoral prostheses

A more common type of characterization in the prostheses market is the following, namely considering energy control:

- **Mechanical passive devices** : these prostheses are non-powered and as such, taking up to 60% of additional energy usage from the patient, and provide reduced mobility, as stated by Hafner et al. in [6]. Moreover, compensatory mechanisms take action to fill up the lack of active power in the leg, primarily these being the back muscles' actuation, which usually results in chronic back pain. This is shown in the study of Jayaraman et al. [7], which mentions how actively powering prostheses may reduce muscle imbalance actuation.

- **Microprocessor-controlled passive devices** : These prostheses implement a microcomputer controlling the knee joint in a passive way to "enhance the patient's gait comfort, safety and cosmesis" as stated in the approach to the design of the Aeyels et al. [8] MPK prosthesis. These are the most popular type of prosthesis currently used by transfemoral amputees.

Figure 1.4: C-Leg from Ottobock [9]

- **Powered devices** which can be further divided into:

  - *Powered knee* : The knee joint is actuated to provide support and motion. These prostheses are heavier than the MPKs since they include an actuation unit which includes a motor powerful enough to aid in high torque requiring tasks such as stair ascent. An example is Fig. 1.5.
  - *Powered ankle* : These prostheses power the ankle actively and allow for greater range of motion. These type of prostheses fit well transtibial amputees as for transfemoral amputees it is better to use a prosthesis that actuates the knee. However, a knee prosthesis and an ankle prosthesis can be attached to provide motion on both joints.
  - *Powered knee ankle devices* : These prostheses actuate both knee and ankle actively and, although they are not a strong presence in the market, there is active research in the field.

    These prostheses are referred to as PKA (Powered Knee Ankle).

Figure 1.5: PowerKnee from Ossur [10]

1.4 Research question

What we are trying to do with the prosthesis design discussed in this thesis is to solve or work around some of the problems affecting current transfemoral prostheses on the market or in literature. These are the 2 main problems we are tackling:

- **Lack of ankle actuation in MPKs** :

  PKA prostheses differ from MKPs primarily because of the active ankle actuation that they provide. One study suggests that actuation of both joints would firstly allow a more physiological type of motion of the prosthetic limb and, secondly, that this could reduce asymmetry in the back muscles activation and overall pain derived by constant use [7], this type of prostheses are of great interest. We would like to have a prosthesis that mimicks well both joints of the leg: current MPKs on the market are very advanced prostheses, but they lack ankle actuation as they rely on passive elastic prosthetic feet.

- **Bulkiness and weight of fully active PKAs** :

  The problem we have to tackle with a multi-joint (knee and ankle) prosthesis is one of trade-off: current PKA prostheses in literature, although much progress is being made, still face a weight and bulkiness problem, as studies such Sup et al. [11] and Mithcell et al. [12] also try to deal with this problem. By utilizing only one motor to actuate both joints instead of two like in current fully active prostheses, we aim to reduce the overall weight and size.

1.5 Motivations for an under-actuated PKA

Tackling the problem by utilizing only one motor to actuate both joints through a smart power transmission design.

The role of hydraulics Hydraulics can serve an optimal solution to the *power transmission* problem. In fact, if we want to reduce the volume, we have to optimize the space that we have available on the leg, keeping into account that this available space should fit in the physiological size of a shank.
Hydraulics predisposition to allowing actuator and power source to reside in different places is the first great advantage. Secondly, double acting hydraulic cylinders serve a good role as actuators as retraction and extension of the piston can allow the attached joint to follow a specific angular trajectory. To reinforce these statements, we can observe that the best selling prostheses on the market use hydraulic actuation as can be seen with the Ottobock C-leg [9].

Figure 1.6: Excavator's hydraulic actuator that allows the joint to rotate around its axis [13]

In addition, hydraulic flows in the actuating cylinders can be modulated by *valves*, which can serve us well in facing forces and velocities modulations.

The under-actuation advantage This particular characteristic allows us to reduce the prosthesis weight and actuate with positive power only during certain phases where it is required. In addition to this, we can note how the walking motion of humans is very energy efficient: this is because walking can be compared to a perpetual falling motion where our COM is displaced forward and the legs swing forward so that we don't fall down, just by braking our descent.

By under-actuating our prosthesis, we have to choose carefully which of the gait phases should be done with positive power and which ones should be carried out passively. We can note that actuating during high force phases in fact wouldn't even be necessary as the stance phase requires positive power by the knee just to hold the body weight and during the *"push-off"* phase. The stance phase can be carried out with the closure of the hydraulic circuit via the valve, so that the hydraulic cylinder remains static in its position and the leg does not flex under the weight of the body. The *"push-off"* phase can be carried out thanks to the help

of the elastic part of the prosthetic foot and, possibly, a percentage of assistance can be given by active power from the motor-pump system. The percentage of assistance isn't as powerful as with a real leg and ankle, but this doesn't matter much as we care much more about reducing weight, bulkiness and noise rather than giving 100% of power which wouldn't be needed.

1.6 Components of the hydraulic circuit

Scheme of the hydraulic circuit This is the concept 1.7 for the hydraulic circuit of the proposed under-actuated prosthesis: This scheme represents the

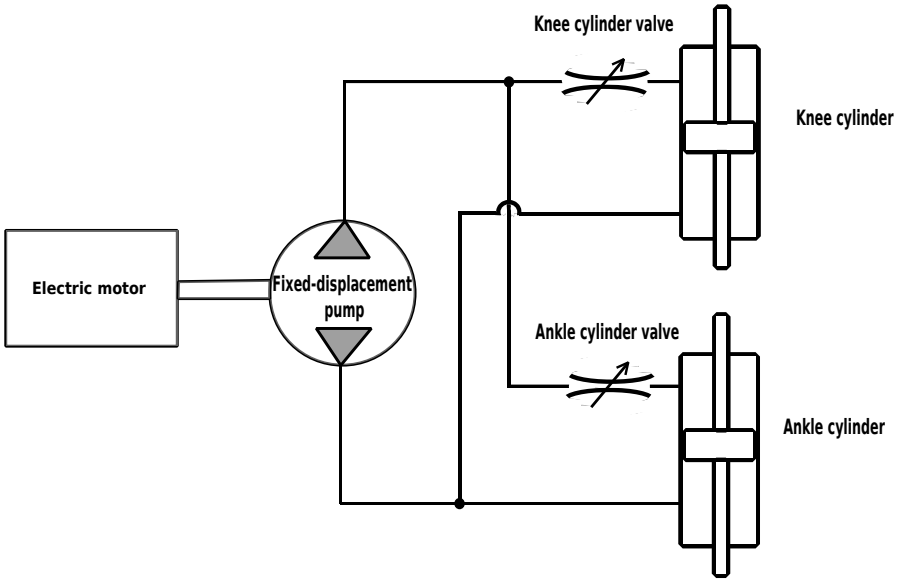

Figure 1.7: Hydraulic circuit of the prosthesis with components

layout of the components of the circuit.

1.6.1 EHA

Albeit electro-mechanical actuation is the most popular and researched type of actuation for lower limb prostheses, electro-hydrostatic actuation can be proposed as a valid alternative, especially when taking into account the dimensions and spacing problems introduced above. It is made up of an electric motor and a fixed-displacement pump, whose respective rotors are rigidly coupled and so have a transmission efficiency that can be approximated to 1. These 2 components are then connected to a hydraulic actuator. Here a brief overview of these 3 parts:

- **Permanent magnet synchronous motor**: In this type of AC(alternate current) electric motor, magnets are attached or embedded into the rotor while copper windings are wrapped up around the teeth of the motor stator. A constant magnetic flux is created by the magnets on the rotor. A varying magnetic field produces a force between the rotor and the stator, thus creating a relative velocity between rotor and stator. The torque is generated by the reaction force generated between the rotor magnets and the windings on the stator teeth. This type of motor has a high efficiency as the magnetic field

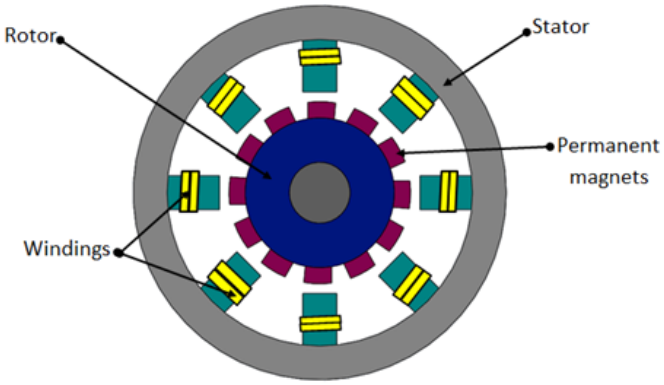

Figure 1.8: Permanent magnets motor [14]

from the magnets acts directly on the air gap, involving low rotor losses.

- **Fixed-displacement pump**: Its primary feature is transforming rotary motion into linear motion thanks to the mean of transmission: the hydraulic fluid. The pump considered for the prosthesis under study is of the gerotor type, which also falls under the internal gears pump category.
  Gerotors are positive displacement pumps in which "the volumetric flow rate is produced by the cyclical suction and delivery phases in the chambers generated by meshing of the gears" as stated in Puliti et al. work[15]. These type of machines are characterized by compactness, high efficiency and low wear with respect to other technologies [16]. These qualities are appreciated for our prosthesis application as we would ideally need a small motor that can spin fast to allow high flows in the hydraulic circuit.
  The fundamental parameter for the hydraulic pump is the displacement D_m, defined by the volume of hydraulic fluid that is able to move over a finite rotary displacement $[cm^3/rev]$.

Figure 1.9: Gerotor pump schematic [17]

- **Hydraulic actuator**: For the scope of this thesis, knee and ankle actuators were opted to be double acting hydraulic cylinders, defined and parametrized by Tessari et al. [18]. These actuators were designed to be backdrivable and have both active and regenerative capabilities, all while being highly-integrated to reach the compactness level required for the application.

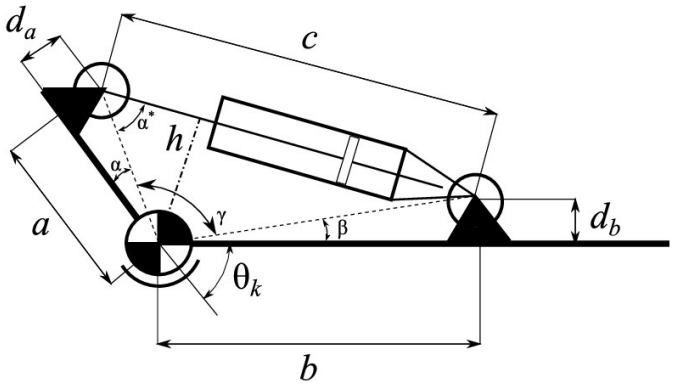

Figure 1.10: Hydraulic actuator schematic [18]

Furthermore it is important to note that such a machine can act both as a motor and as a generator (during braking periods) thanks to the back EMF generated by Faraday's law in the electric motor. The design and characterization of a motor-pump unit for energy regeneration has been studied by Galluzzi et al. applied to shock absorbers [19], while Tessari et al. defined a parameters characterization of the EHA for lower limb prosthetic applications [20]. Such principles can be similarly applied to our under-actuated prosthesis thanks to this literature background.

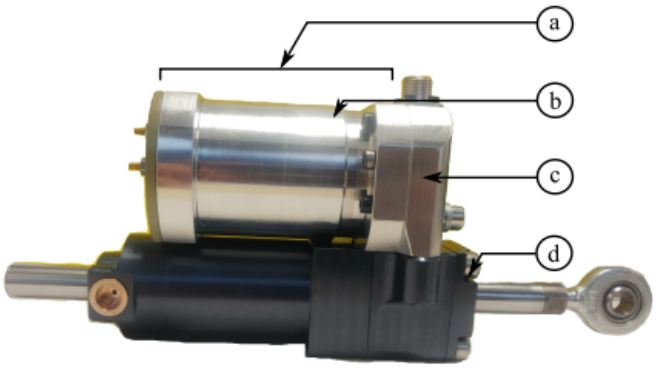

Figure 1.11: EHA with one hydraulic actuator (a) case, (b) electric motor, (c) gerotor pump, (d) hydraulic cylinder [18]

The utilized concept and model for EHA in lower limb prosthesis applications is discussed by Tessari et al. in [20], where a test rig is designed and used to achieve experimental results proving that the EHA, thanks to control strategies, is able to to precisely reproduce bio-mechanical knee trajectories in three conditions: level walking, step ascending and step descending. Moreover efficiencies were also validated. In addition in [20] it is showed that this actuator can have mass and dimensions appropriate for such application.
These studies are the groundwork and base of the prosthesis in development.

1.6.2 Valves

These components are used to control the flow in the hydraulic cylinders. By shutting a valve we can ideally block the cylinder's movement, however, in reality, a small leakage is always present.
The type of valves ideally used in the prosthesis in discussion are flow control rotary valves.

Chapter 2

Theoretical analysis

2.1 Data and literature analysis

Introduction To have a clear idea of the angles, velocities and forces into play during the gait cycle we must consider a reliable source of such data. Lencioni et al.. provides just that [21]. This dataset comprises of data from 50 subjects: for each, kinematic, kinetic and EMG data for the ankle, knee and hip joint are present, taken during different tasks as walking, stair ascending and descending. Alongside this information also name, age, height, weight, sex and side (left, right) of the measurement.
Initially, the following data of interest was acquired for the hip, knee and ankle joint: As age and anatomical proportions differ in this dataset (to include multiple

Angles	Moments	Powers
θ_{knee}	M_{knee}	P_{knee}
θ_{ankle}	M_{ankle}	P_{ankle}
θ_{hip}	M_{hip}	P_{hip}

Table 2.1: Data extrapolated from the data-set

type of subjects) it is important to make an average of this data as to base the sizing of the components on requirements that could fit the average person. To accomplish this, an average subject was taken into account (50^{th} percentile male population):

- **Height** : 175 cm
- **Weight** : 78.5 kg

Moreover, geometries and anatomy of the body are also fundamental data, which

were found in [22]. Here, the average subject's measurements can be retrieved.

Averaging This is the data figure containing angles, momenta and powers for knee and ankle joints.

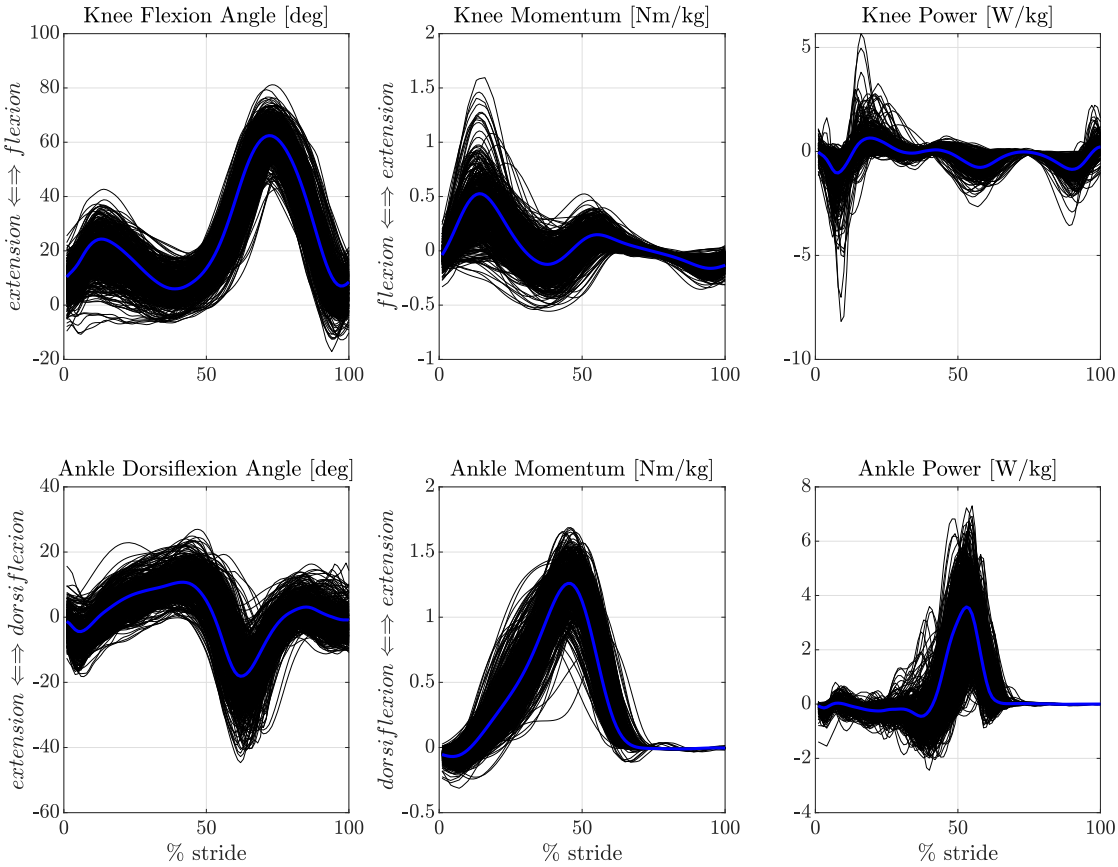

Figure 2.1: Data from 50 subjects: black lines → each subject data, blue lines → average of all the subjects [21]

Ankle angle offset In this dataset the ankle angle is presented with an initial condition of about $-20°$ at the start of the gait cycle and this offset from the $0°$ protracts for the whole stride. However, the plantar plane is perpendicular to the tibia/fibula axis at "heel-down" position (which denotes the start of the gait cycle). This offset is due to how the rotation (flexion and extension) is defined in the dataset, which references [23][24] as bases in the definition of JCS (joint coordinate system) for knee, ankle and hip joint.

Wu et. al [23] defines the rotation of the ankle joint around the *Z axis* of **Fig. 2.2**. Such axis is slanted with respect to the ground and not parallel (while the calcaneus coordinate systems has the *z axis* parallel to the ground).

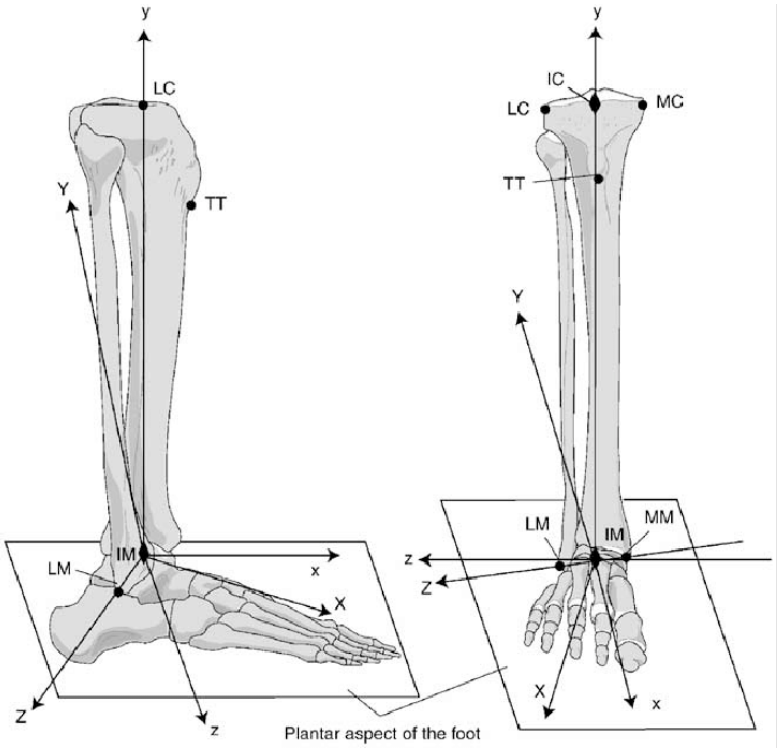

Figure 2.2: Illustration of the tibia/fibula coordinate system (XYZ) and the calcaneus coordinate system (xyz) with the ankle joint complex in the neutral position [23].

The angular difference θ_{offset} between *X axis* (tibia/fibula coordinate system) and *x axis* (calcaneus system) is around 20°. This value was approximated by noting that the X axis follows the dorsum of the foot and so that θ_{offset} is similar to the angle that the dorsum has with the ground (alternate internal angles).
After that, by evaluating the foot measures of our average subject, this offset was estimated (20°) and added to the extrapolated data from the data-set.
Ultimately, this was done to define the ankle angle as positive during dorsiflexion, and negative during plantarflexion, as seen in Fig. 2.3.

Biomedical notation and right hand rule notation for angles It is important to note that there are discrepancies between rotation **sign** convention in the medical world and engineering world, in fact, for medical purposes it is more useful to define motion by extension and flexion, while for kinematic and

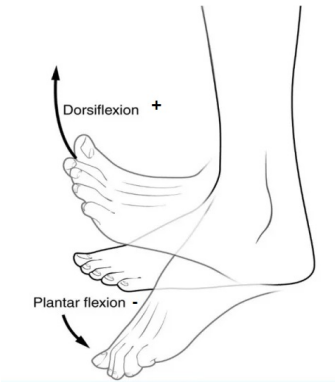

Figure 2.3: Ankle angle definition [25]

dynamic analysis we would like all angles to follow the right hand rule, which states: counter-clockwise motion → positive angle, while, clockwise motion → negative angle.
For this purpose, the *extension* ⟸⟹ *flexion* notation was used for angles in Fig. 2.1, while here is presented the "right-hand rule" graph, which was then used for following calculations

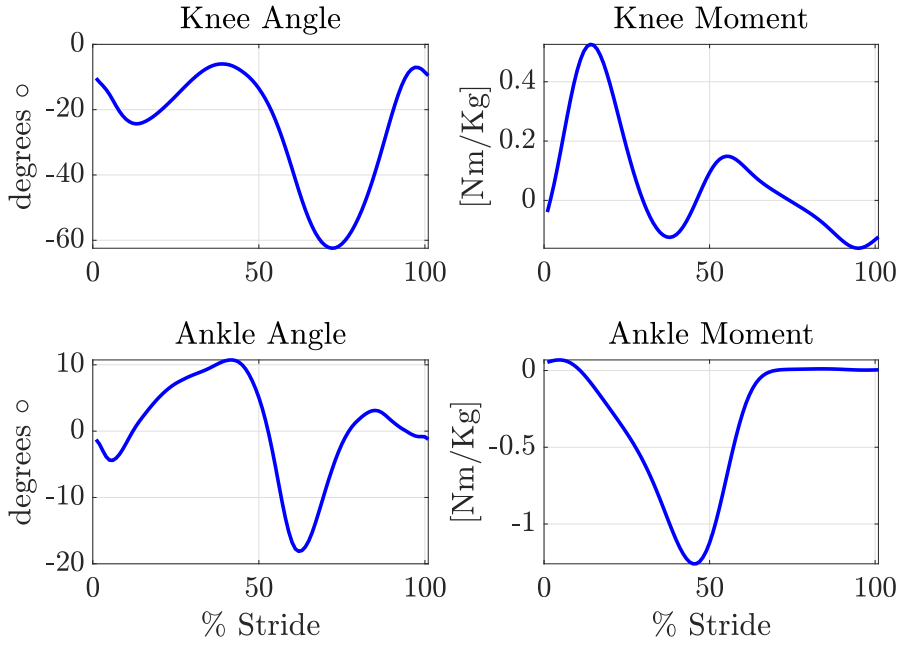

Figure 2.4: "Right-hand rule" angles and moments.

As we can see by Fig. 2.4 the knee angle is mostly negative as the neutral position

is defined as the kinematic singularity of the straight leg.
The ankle moment is negative as the "push-off" phase corresponding to the peak is carried out by pushing the foot against the ground in a counter-clockwise motion.

2.2 Kinematic analysis

2.2.1 Velocities

Derivation of the position to obtain the velocity Calculating the forward discrete derivative of the knee and ankle trajectory outputs the respective joint angular velocities. Two cases were studied: an average gait velocity of 4.4 km/h and a fast gait of 6 km/h. The discrete derivatives were calculated in the following way:

$$\omega_j = \frac{\theta_j(t+1) - \theta_j(t)}{\Delta t}$$

The time steps Δt were calculated as:

$$\Delta t = \frac{l_{avg}}{v_{avg}}$$

- $l_{avg} \rightarrow$ average length of the strides of all subjects
- $v_{avg} \rightarrow$ average speed of the strides of all subjects

The resulting angular velocity for an average speed of 4.4 km/h over the whole stride are the following:

- $\omega_{K_{max}} = 56.6$ rpm
- $\omega_{A_{max}} = 42.4$ rpm

The resulting angular velocity for an fast speed of 6 km/h over the whole stride are the following:

- $\omega_{K_{max}} = 62.8$ rpm
- $\omega_{A_{max}} = 47.1$ rpm

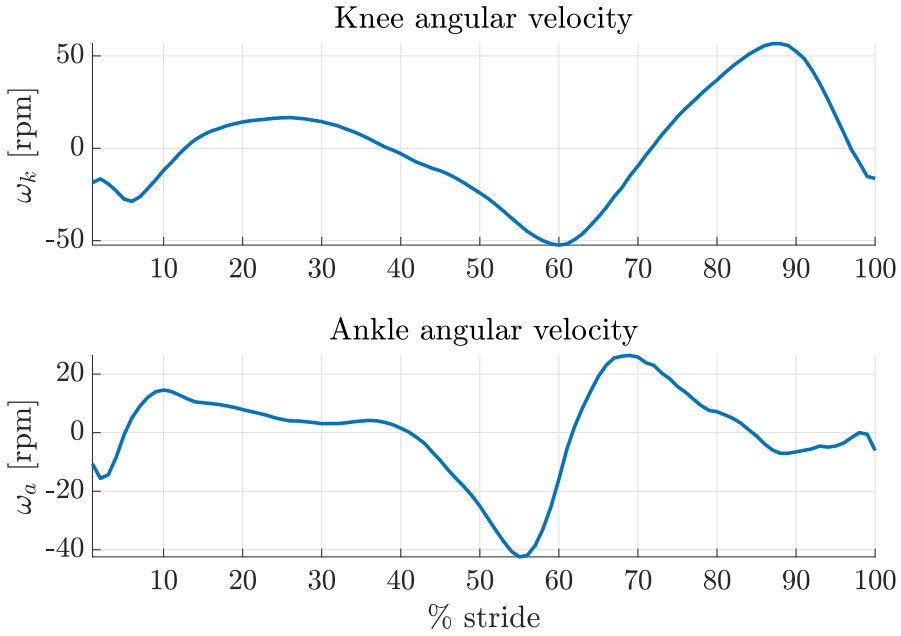

Figure 2.5: $4.4km/h$ walk angular speed for knee and ankle joint.

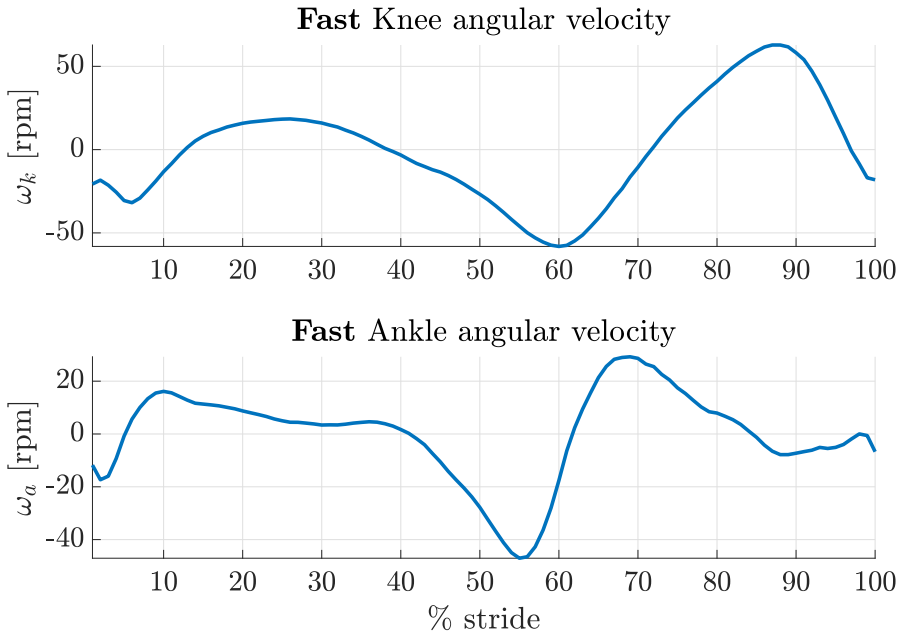

Figure 2.6: $6km/h$ walk angular speed for knee and ankle joint.

2.2.2 Accelerations

Derivation of the velocity to obtain the acceleration Calculating the forward discrete derivative of the knee and ankle angular speed outputs the respective joint angular accelerations. Only the fast walk case was taken into account as it is the more interesting in our case. The discrete derivatives were calculated in the following way:

$$\dot{\omega}_j = \frac{\omega_j(t+1) - \omega_j(t)}{\Delta t}$$

The time steps Δt were calculated in the same way as in the previous section. The resulting angular accelerations for a fast walk speed of 6km/h over the whole stride are the following:

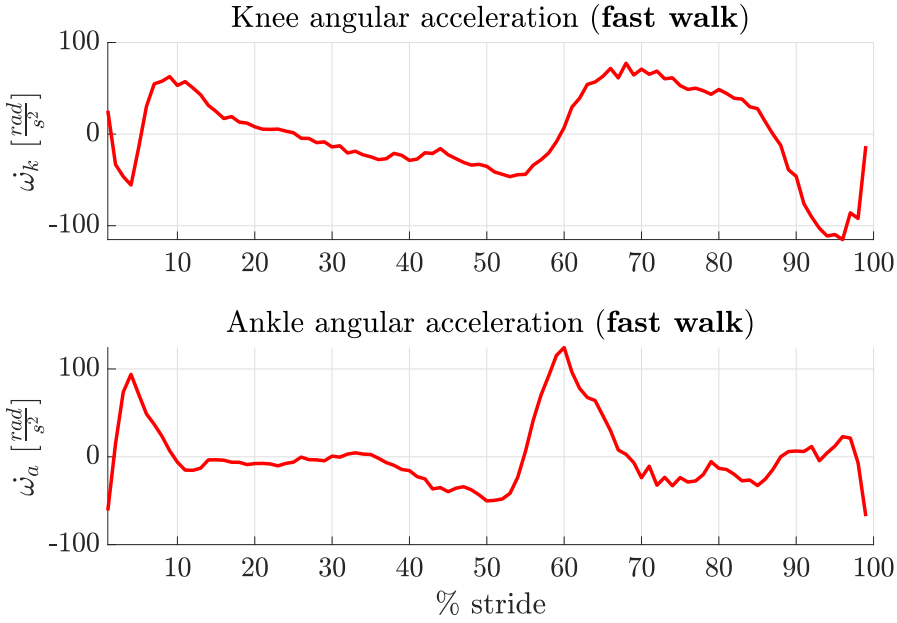

Figure 2.7: $6km/h$ walk angular acceleration for knee and ankle joint.

- $\dot{\omega}_{K_{max}} = 115.1\ rad/s^2$
- $\dot{\omega}_{A_{max}} = 124.4\ rad/s^2$

2.2.3 Sizing of the knee components

Objective

1. Determine which configuration is better for the cylinders' positioning.
2. Calculate the lever arm that both knee and ankle cylinders create with the actual joints.

The main task of this section was to come up with a good trade-off between comfort, aesthetics and performance. The lever arms (that can be seen in Fig. 2.8) are the means of transformation of the joint torques to the cylinder forces, so these have to be carefully chosen to satisfy our requirements. All of this has to be done by keeping into account physiological and anatomical limitations.

Prosthesis concept, 1^{st} configuration The initial concept for the prosthesis was to have the hydraulic cylinder positioned on the back of the knee and one on the back of the ankle, as seen in Fig. 2.8. This is motivated by the fact that, anatomically, for the ankle, our Achilles tendon and calf muscles are positioned behind the tibia bone, moreover this resulted in a good performance in terms of comfort and lever arm with respect to other configurations. This scheme was the one we went with for the prosthesis development.

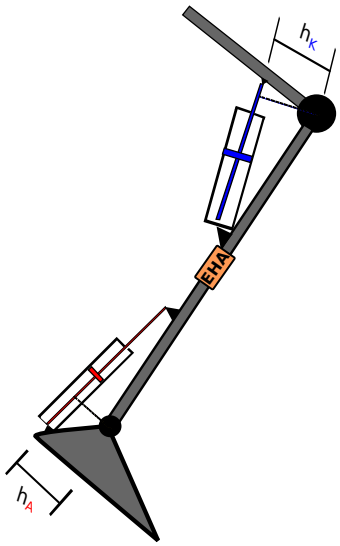

Figure 2.8: Scheme of the prosthesis concept (note that the proportions are not realistic); h_K and h_A are the lever arms that the forces on the cylinders have with the joints.

Alternative configurations Two alternative configurations were investigated for the positioning of the ankle cylinder. Performances (in terms of lever arm) were similar to the ones of the 1^{st} configuration, we deemed them too uncomfortable, as a cylinder of discrete volume and lever arm takes up a lot of space. Moreover, it seemed that a cylinder on the front of the foot would be too noticeable aesthetically speaking, so we discarded these configurations.

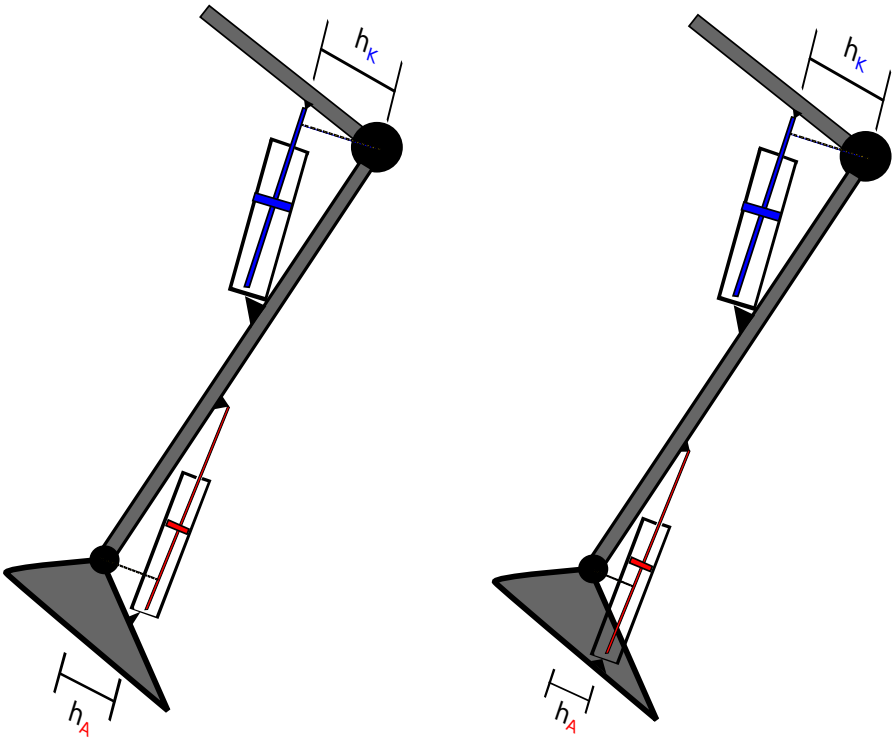

Figure 2.9: Alternative configurations that were investigated.

Sizing of the 1^{st} configuration

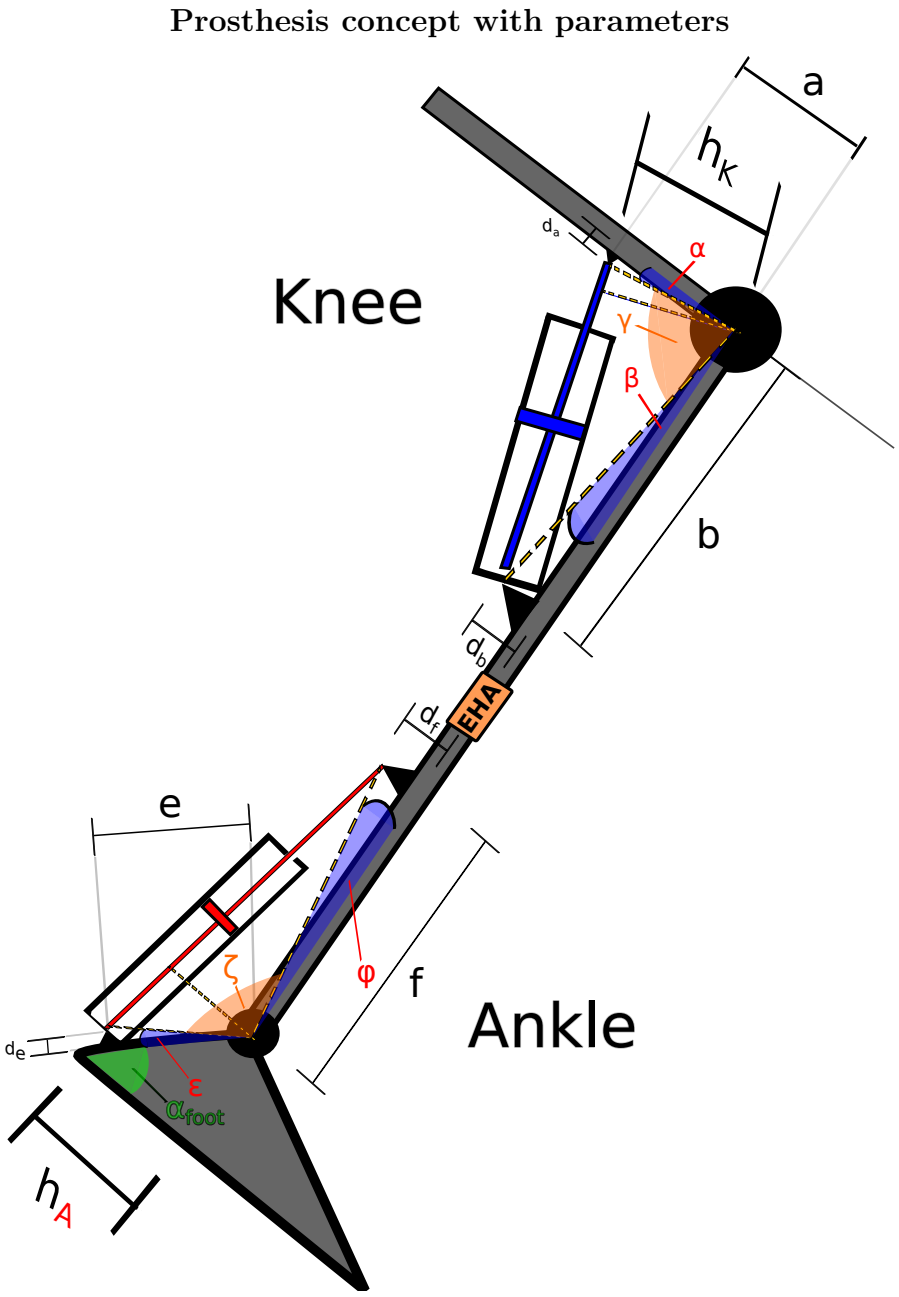

Figure 2.10: Scheme of the prosthesis concept with variables for calculation of the lever arm depending on the point of attachment of the cylinders and height of the cylinder with respect to the axial length.

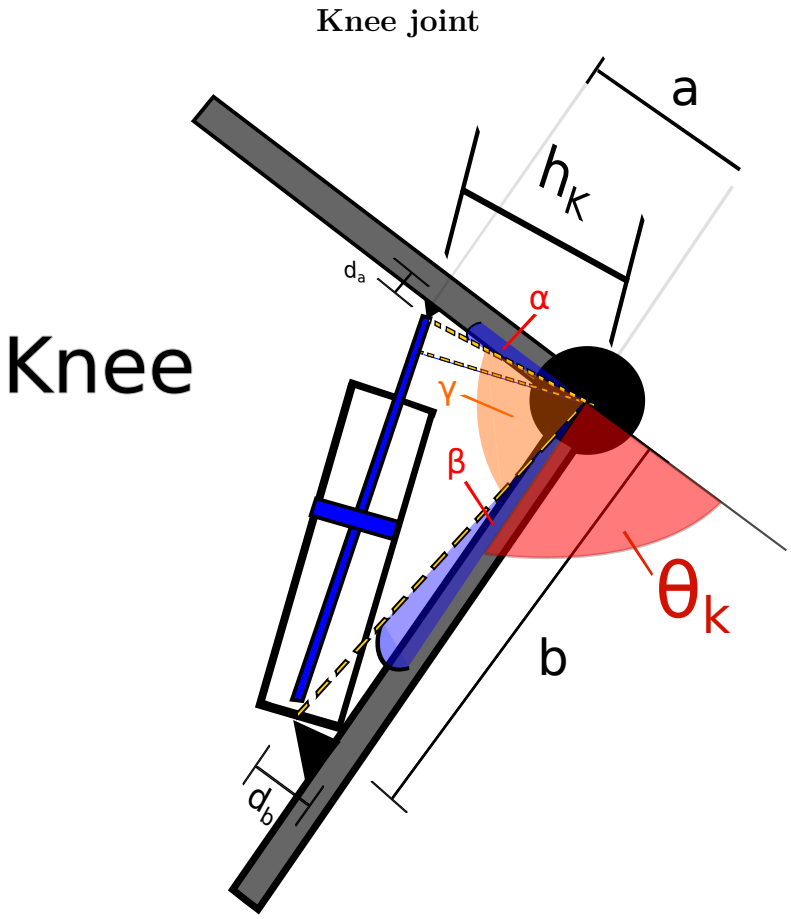

Figure 2.11: Scheme of the knee joint with the hydraulic cylinder and parameters.

Geometric sizing of the knee We want to define the lever arm in function of the positioning of the knee cylinder. Firstly, we define the angles:

$$\alpha = \arctan \frac{d_a}{a} \ , \ \beta = \arctan \frac{d_b}{b}$$

$$\gamma = \pi - \theta_k - \alpha - \beta$$

$$A = \sqrt{a^2 + {d_a}^2} \ , \ B = \sqrt{b^2 + {d_b}^2}$$

$$C = \sqrt{A^2 + B^2 - 2 \cdot A \cdot B \cdot \cos\gamma} \text{ ,where C is the cylinder variable length}$$

$$\bar{\alpha} = \arcsin \frac{B}{C} \cdot \sin\gamma \text{ , which is the adjacent angle of } \gamma$$

and finally

$$\boldsymbol{h_K = A \cdot \sin \bar{\alpha} \Rightarrow}\ \text{knee joint lever arm}$$

For the knee joint, the geometries were optimized following [18] to **minimize** the lever arm, so to have a knee joint that is as backdrivable as possible.

The following values were selected for the knee:

Table 2.2: Optimized values for the knee cylinder positioning.

a	20	mm
b	150	mm
da	34	mm
db	25	mm

Results These values gave rise to the following lever arm and stroke :

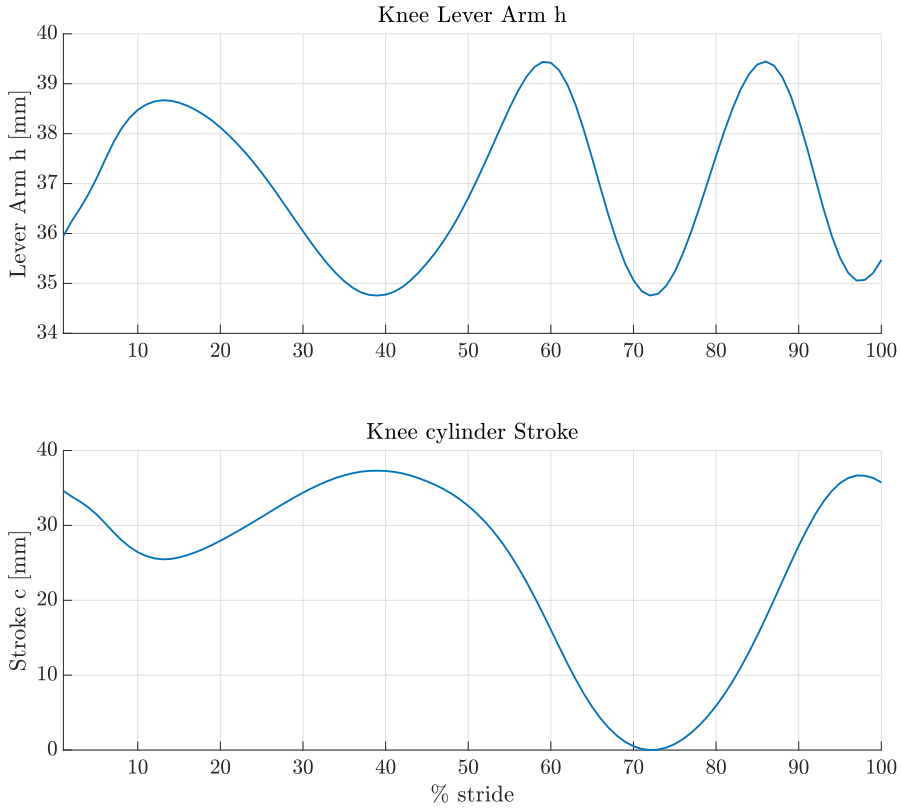

Figure 2.12: Knee lever arm and cylinder stroke during the whole stride.

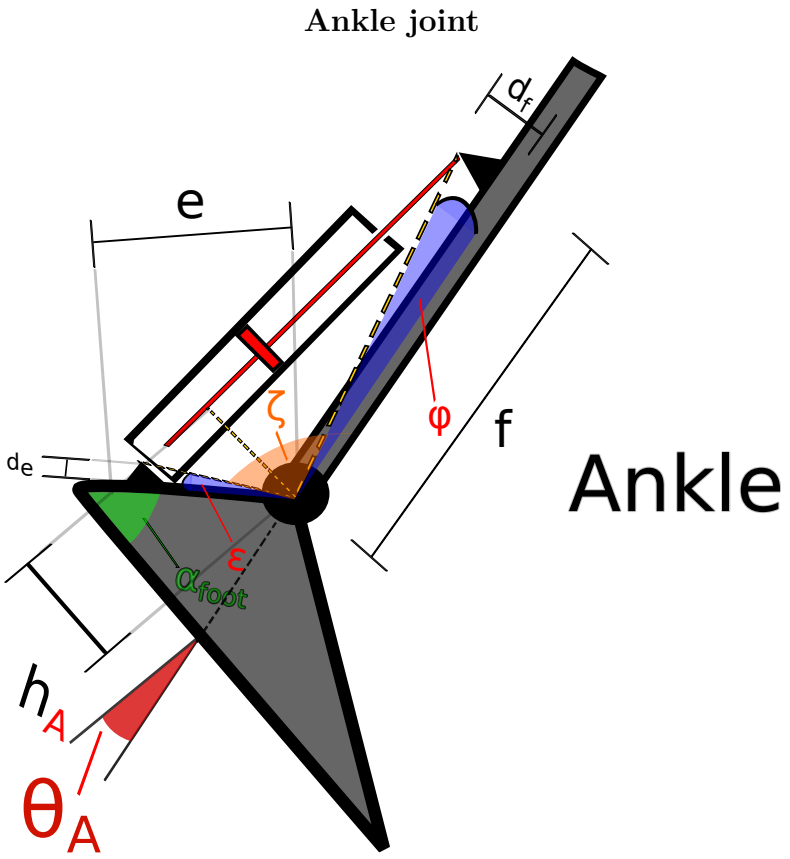

Figure 2.13: Scheme of the ankle joint with the hydraulic cylinder and parameters.

Geometric sizing of the ankle We want to define the lever arm in function of the positioning of the ankle cylinder on the tibial part and on the heel. Firstly, we define the angles:

$$\epsilon = \arctan \frac{d_e}{e} \ , \ \phi = \arctan \frac{d_f}{f}$$

$$\zeta = \pi/2 + \theta_A + \alpha_{foot} - \phi - \epsilon$$

$$E = \sqrt{e^2 + {d_e}^2} \ , \ F = \sqrt{f^2 + {d_f}^2}$$

$$G = \sqrt{E^2 + F^2 - 2 \cdot E \cdot F \cdot \cos\zeta} \ , \text{ is the cylinder variable length}$$

$$\bar{\phi} = \arcsin \frac{E}{G} \cdot \sin\zeta \ , \text{ which is the adjacent angle of } \gamma$$

and finally

$$\boldsymbol{h_A = F \cdot \sin \bar{\phi} \Rightarrow}\ \text{ankle joint lever arm}$$

For the ankle joint, the geometries were optimized to **maximize** the lever arm, so to reduce as much as possible the forces on the cylinder. This depended on the positioning of the cylinder, on the height of the attachments d_e d_f and on the angle that the heel forms with the ground α_{foot}. This value was assumed to be 60° as, depending on the type and design on the prosthetic foot, this value could change.

The following values were selected for the ankle: The **e** value was chosen inside

Table 2.3: Optimized values for the ankle cylinder positioning.

e	100	mm
f	160	mm
de	20	mm
df	35	mm

the physiological bounds of the ankle joint-heel distance, while **f** was chosen to be less than the half tibia length.

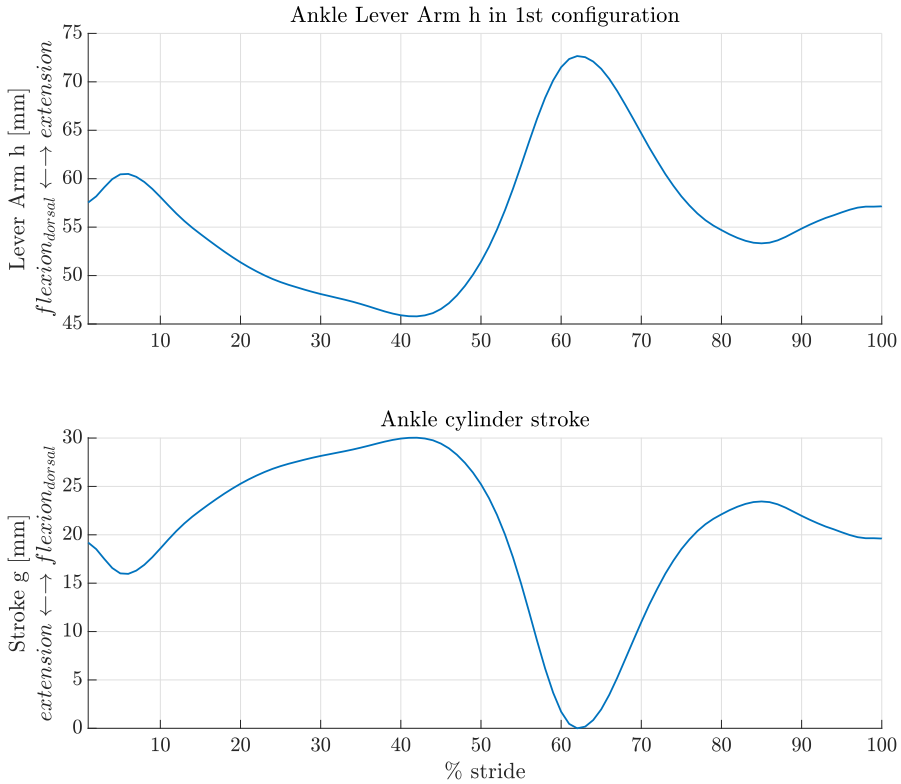

Figure 2.14: Ankle lever arm and cylinder stroke during the whole stride.

2.3 Force-Speed relation

To determine the active power phases of the gait cycle one has to look at the signs of forces and velocities.
The torque angular velocity graph can help us understand which phases of the cycle reside in which quadrant and realize whether there are phases with negative torques and positive velocities, where energy regeneration principles could be applied.

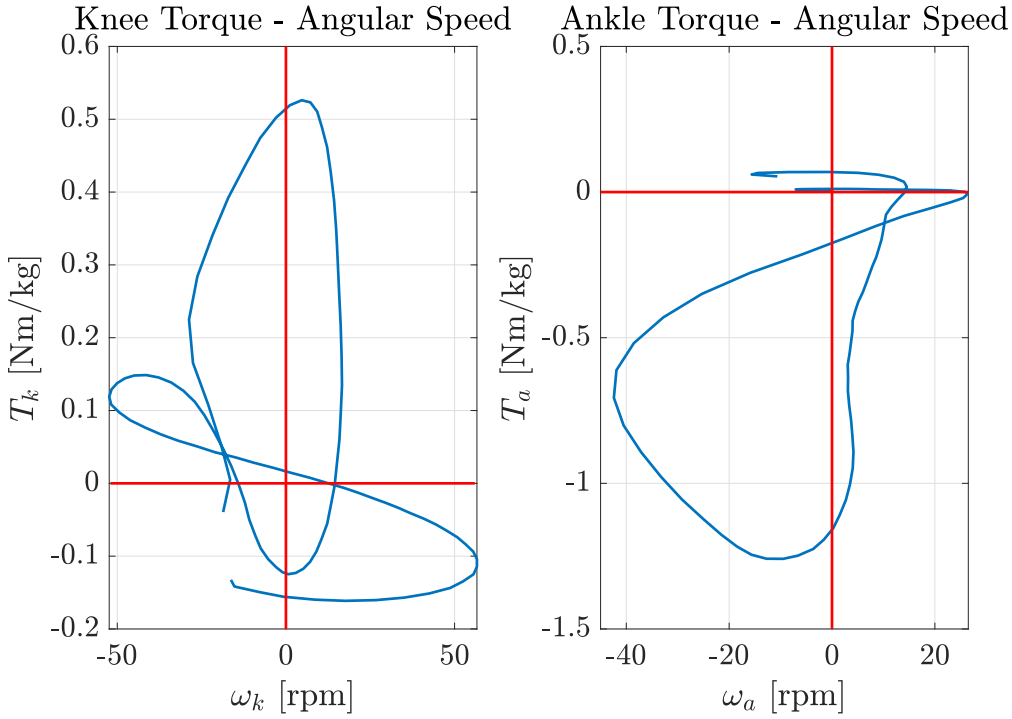

Figure 2.15: torque angular speed graph. Notice that both of these graphs follow the right hand rule, meaning that the direction of the torque and of the velocity is consistent with said rule

As we can see in Fig. 2.15 the II and IV quadrant are the ones where the knee and ankle work with negative power and where the Swing phase resides. The IV quadrant could be suited to apply energy regeneration principles (since in the II quadrant the gravity is working against the leg).

2.4 Forces and speed on cylinders

Forces By dividing the torques on the joints by the lever arm we get the forces on the cylinders:

$$F_{cylinder_K} = \frac{T_K}{h_K} \ , \ F_{cylinder_A} = \frac{T_A}{h_A}$$

where T are the torques on joints (that can be seen in Fig. 2.1) and h are the lever arms (in vector form).

Speed Contrary, the linear speed (Fig. 2.17) of the cylinders are found by multiplying the angular velocities by the lever arm.

$$v_{cylinder_K} = \omega_K \cdot h_K \ , \ v_{cylinder_A} = \omega_A \cdot h_A$$

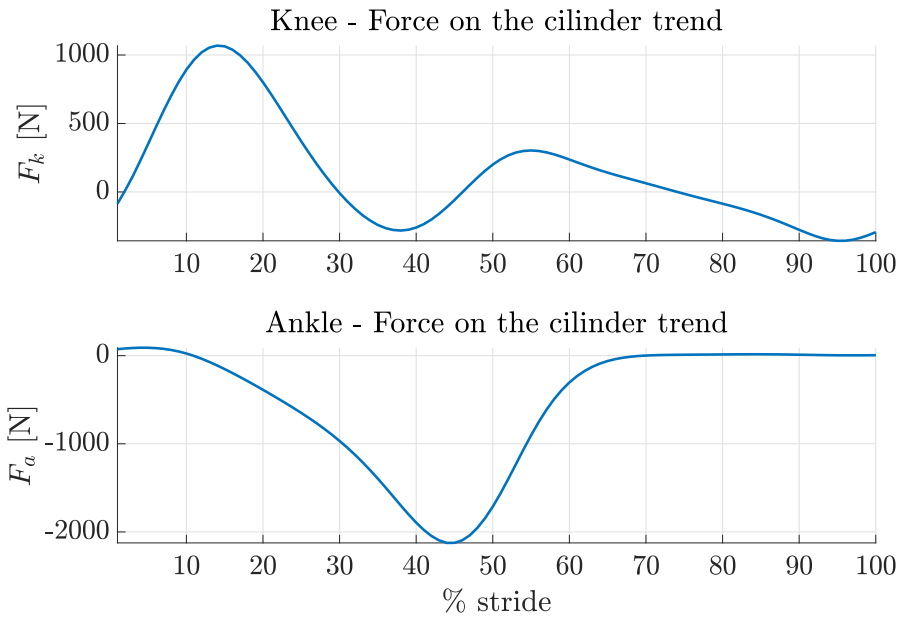

Figure 2.16: Force on knee and ankle cylinder

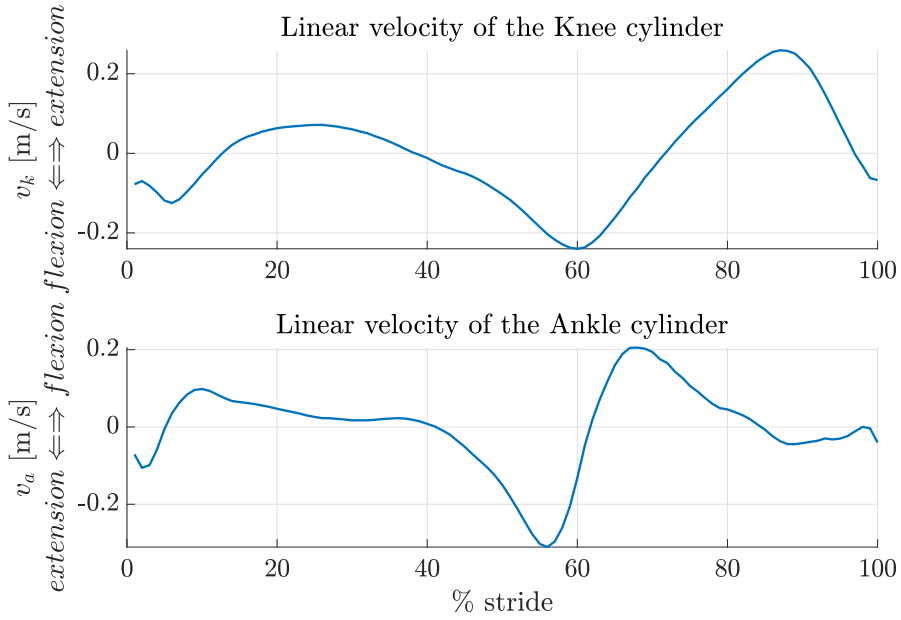

Figure 2.17: Linear velocity of knee and ankle cylinder

2.5 Sizing of the circuit components

2.5.1 Swing sizing

One of the main objectives of the prosthesis in study is to be light-weight. This is achieved by optimization of the components power and by their respective weight. A prosthesis with a heavy and bulky actuator would go against a comfort-based design, so we have to be careful in the sizing of our components.
As can be seen in Fig. 2.16 the forces in the stance phase (0-60 % of the stride) are quite high for both knee and ankle, since the knee "brakes" and supports the weight of the body and the ankle activates during the push-off, propelling the leg up and forward for the swing.
Emulating such forces with an hydraulic actuator powered by a motor-pump unit is possible, but would require a powerful motor with at least 2 Nm of peak torque, or a higher transmission ratio. Commercial high-end motors of such torque (e.g., [26]) are bulky and heavy for our scope, moreover they can only reach limited speeds which don't allow us to pump enough fluid in the chambers of the cylinders during the swing phase.
One could consider the use of a gearbox/reducer between motor and pump to achieve the high forces requirements. This, nonetheless, would decrease the knee backdrivability and efficiency (Wang et al. [27]), in addition to having maximum speed problems.

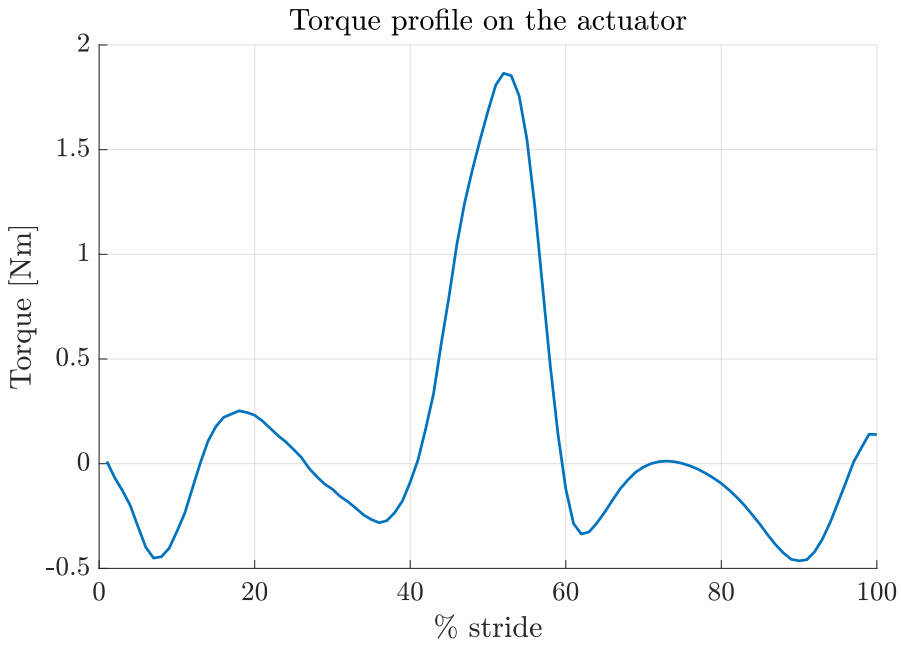

Figure 2.18: Torque we would need at the motor to make a full-active prosthesis

So we have a trade-off that we need to consider. *A reasonable choice for our design is to actuate the leg only during the swing phase, while using the valves only to regulate the prosthesis during the stance phase.*
This brings us to consider the low forces and high velocities that occur during the swing phase and so to aim our design and sizing towards satisfying the high velocity requirements. This was also reflected in the cylinders positioning. A backdrivable knee allows the prosthesis to swing more freely, while an ankle cylinder with great arm allows to reduce forces on the actuator, so to possibly partially assist during high-force phases.

2.5.2 Assumptions on component efficiency

The following efficiencies were assumed for the various hydraulic circuit components:

- $\eta_{cylinder} = 0.9$
  This is the approximated average between mechanical and hydraulic efficiency.

- $\eta_{pump} = 0.55$
  This was kept low with respect to the maximum efficiency calculated by the Tessari et al. work [28] and Puliti et al. work [29] (which are some of the groundworks for this thesis) since the working points of the pump (seen

experimentally) resulted in a mix of high and low efficiency points. In addition, a conservative approach was preferred.

- $\eta_{motor} = 0.75$
  Although the maximum efficiency from the TQ-Motors datasheet [30] is 88%, we remained conservative to take into account non-idealities that might not be included in the model and calculations.

While for the motor-pump attachment the efficiency was assumed to be 1 as it is a rigid link with basically zero losses.

2.5.3 Hydraulic double-acting cylinders

The cylinders used in the prosthesis come from the Tessari et al. work [18]. The main value that we need is the surface area of the piston, which is considered equal for both faces of the piston and equal for both cylinders.

$$A_K = 3.778 \cdot 10^{-4} m^2$$

$$A_A = 3.778 \cdot 10^{-4} m^2$$

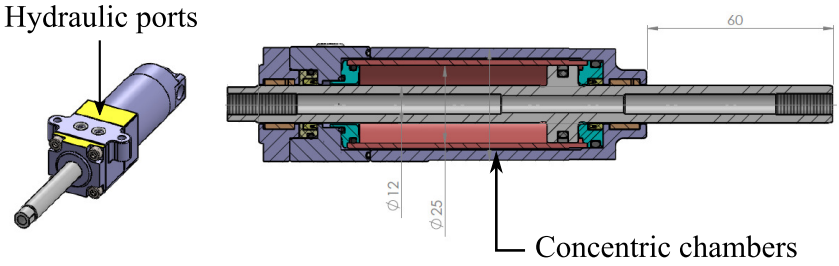

Figure 2.19: Hydraulic knee cylinder [18]

Flows inside the cylinders

The piston area allows us to calculate the flow inside the cylinders during the stride:

$$Q = v_{cylinder} \cdot A_{cylinder} \cdot \eta_{cylinder}$$

where $v_{cylinder}$ is the linear velocity of the piston as in Fig. 2.17.

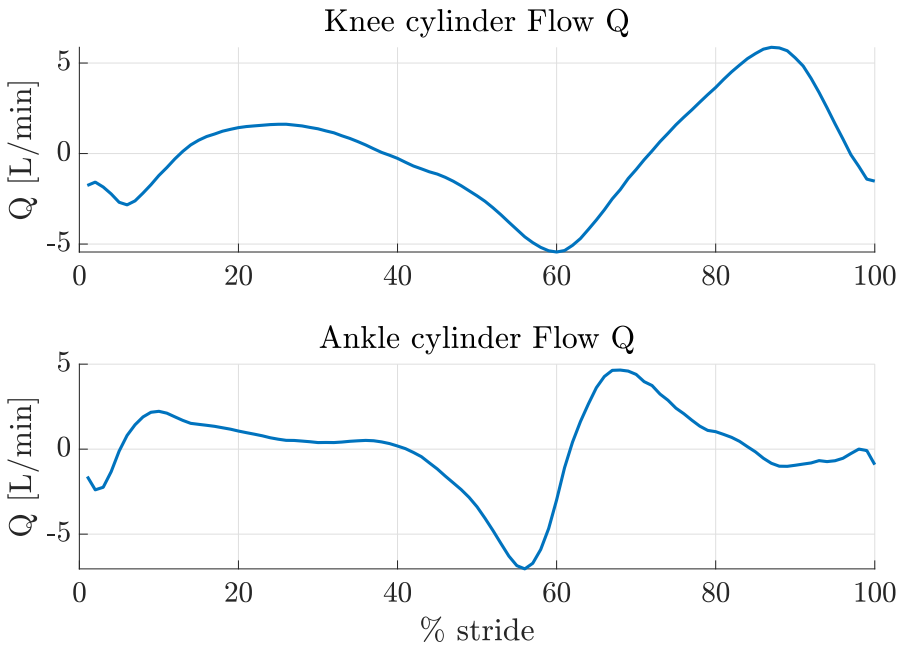

Figure 2.20: Flows in [L/min] inside each cylinder, the higher the velocity, the higher the flow

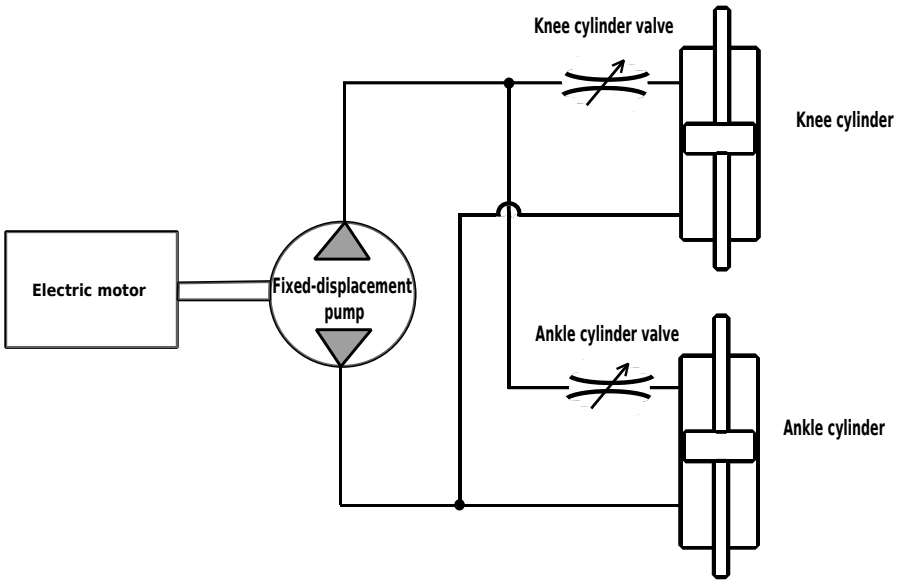

Figure 2.21: Hydraulic circuit of the prosthesis with components in the direct configuration

2.6 Sum of flows

The flow that the hydraulic pump sees is the sum at the upper node (Fig. 2.21) of the two flows coming from the hydraulic cylinders.

We have to be careful when summing the flows as it is not a simple sum; the signs of the velocities of the cylinders have to be taken into account. For these two configurations, the following formulas output the sum at the upper node:

Direct configuration

$$Q_{tot} = -sign(v_{cylinder_K}) \cdot |Q_K| - sign(v_{cylinder_A}) \cdot |Q_A|$$

which gives rise to the following trend:

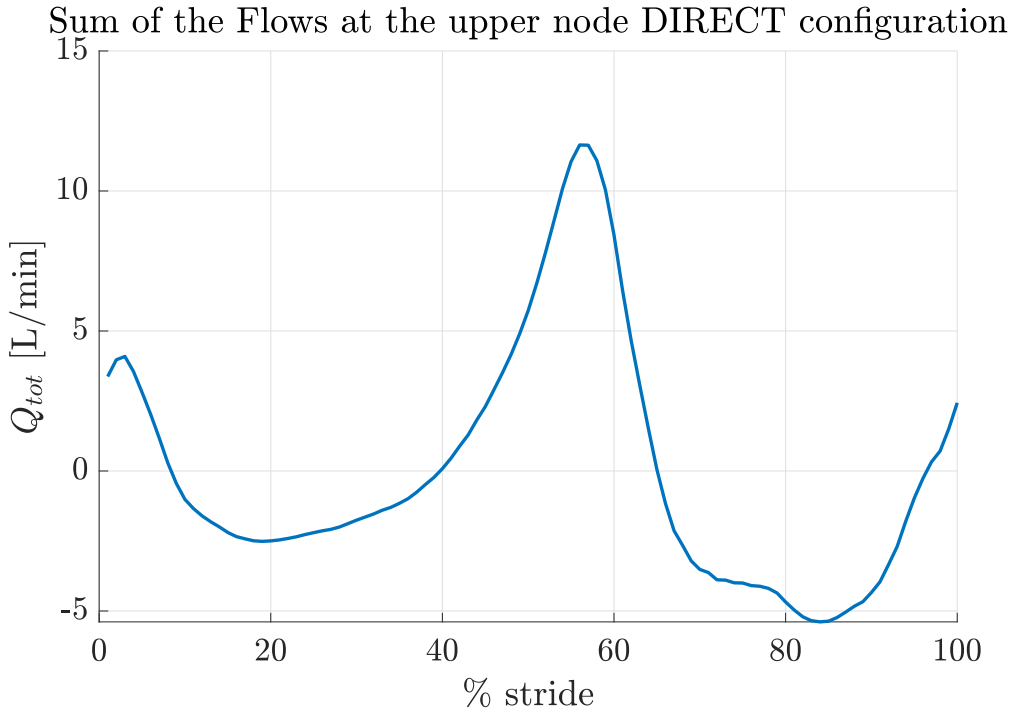

Figure 2.22: Sum of the flows in a direct configuration

Inverse configuration

$$Q_{tot} = sign(v_{cylinder_K}) \cdot |Q_K| - sign(v_{cylinder_A}) \cdot |Q_A|$$

which gives rise to the following trend:

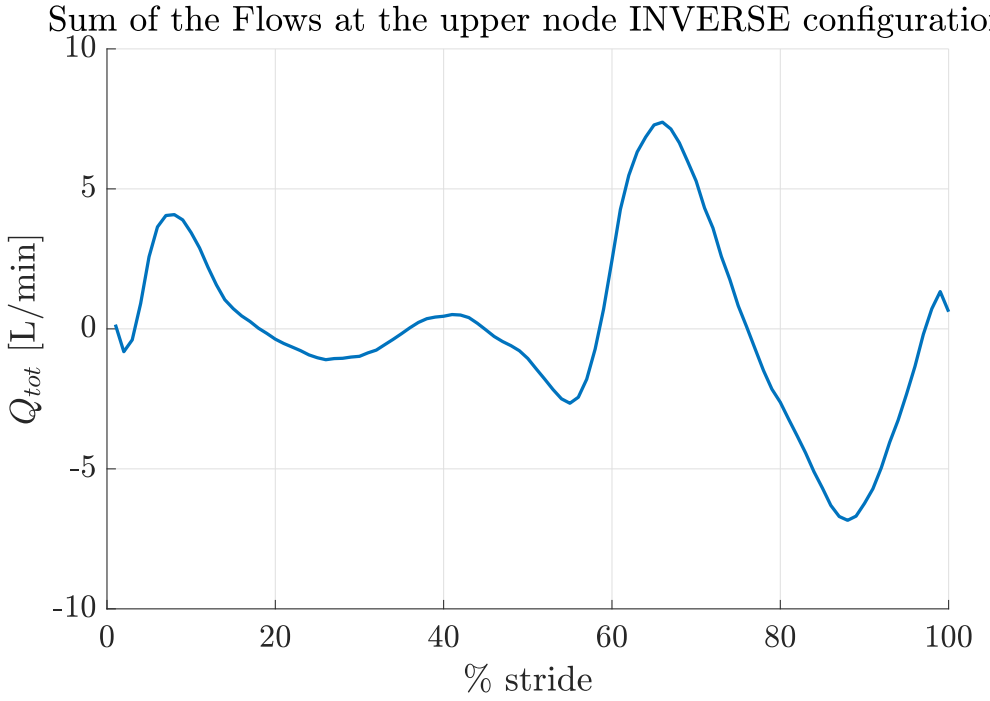

Figure 2.23: Sum of the flows in an inverse configuration

Discussion As we can see by Fig. 2.22 and Fig. 2.23 the maximum flow in the direct configuration is greater with respect to the maximum in the inverse configuration. This, however, is acceptable as the direct configuration is necessary for kinematic purposes.
In fact, we have that, to the flexion of the knee, often corresponds a plantarflexion of the ankle, especially in the swing phase. Then, by inputting a positive flow in the upper node, we can achieve this, but only if we have a direct configuration of the circuit. With an inverse configuration, the contrary would happen.

2.7 Pump sizing

The pump in consideration is a fixed-displacement one of the gerotor type as discussed in the **Background** chapter. Fixed-displacement means that the fluid displacement does not vary, although is varies slightly during a whole rotation. The main parameter that we need to determine is the flow displacement. This can be obtained by the following formula:

$$D_m = \frac{Q}{w_{pump}}$$

We consequently need to fix an appropriate ω_{motor} (which is equal to ω_{pump} as the two are rigidly connected).

Speed choice Taking as a reference the ilm50x08 motor [30], we can see that the maximum speed is 6850 rpm. However, it is more cautious to not approach this limit speed. As such, to determine the D_m parameter, a middle-range speed was chosen:

$$\omega_{motor} = \omega_{pump} = 3600 \text{ rpm}$$

This, in addition, leads to a displacement value which is in a reasonable range (thinking about dimensions and positioning of the pump as well). This value could possibly be augmented to lower the D_m, as we are quite far from the limit speed. *Note*: This speed is achieved by a star-serial connection of the motor different configurations can lead to higher speeds.

Consequently we have that our displacement:

$$D_m = \frac{Q_{max}}{w_{motor}} = 3.23 \text{ cc/rev}$$

where $Q_{max} = 11.64$L/min is the maximum amount of flow that the pump could move. This, however, is not the practical maximum (as in Fig. 2.22) because this peak occurs during the stance phase, which is carried out through the use of the valves only; this reflects in a smaller range of motion with respect to the physiological one → smaller angular velocities of the joints → lower flows.
This fact, added to the simulation results that will discuss later, leads us to be able to assume a maximum flow of:

$$Q_{max} = 7.38 \text{ L/min}$$

and consequently

$$D_m = \frac{Q_{max}}{w_{motor}} = 2.05 \text{ cc/rev}$$

which is the value we considered for the pump displacement.

Naturally, an in-depth design of the pump (geometric parameters, losses, etc..) is due for such an application. However, for the scope of this thesis, this is omitted, as the focus is on the general capabilities of the prosthesis .

2.8 Motor sizing

Directly connected to the hydraulic pump is the electric motor. The fundamental parameter that we have to dimension for this component is the rated torque T_m. This arises a trade-off between power and dimensions of the motor unit, as we want

it light and powerful enough for our application.
To understand the magnitude of the torques into play we need to calculate the inertia that the knee and ankle joint see during the swing phase (swing sizing).

2.8.1 Inertia calculation

During the swing phase the leg does not touch the ground so there are no reaction forces. The only resistance seen by hip, knee and ankle joints are the inertiae of the limb segments. These values were retrieved in [31].

Anatomical measurements Considering our fifty-percentile male subject (H: 175 cm , M: 78.5 kg):

- **foot weight**: $1 + 0.6$ kg, where 0.6 kg is the weight of an average shoe.
- **prosthesis weight**: 3 kg
- **prosthesis COM**: 49.8/2 cm where 49.8 cm is the knee-heel distance. This distance is half the length of the knee-ground distance.

These values are conservative since for the COM the components could be moved closer to the knee joint to reduce the inertias. Same thing for the weights, as a total weight of 4kg for the whole prosthesis (without the shoe) is an estimation based on previous prosthesis designs. An average tibia+foot in a physiological leg weighs about 5kg. The lighter end of transfemoral prostheses weigh about 2kg. An average between these 2 would be 3.5kg

Simple pendulum assumption

Initially, the assumption that the leg movement during swing could be the one of a single pendulum was made. This assumption brings us to consider the whole prosthesis as a point mass (tibial and foot part together) connected to the knee joint by a zero mass rod. This assumption is not so realistic since, during walk, the hip movement contributes a lot to the leg swing. Moreover, it is the body inertia which propels the limbs forward. However, it was deemed satisfactory as an initial estimation of the inertiae into play.

Calculations

$$I_{K,A} = (M_{foot} + M_{prosthesis}) \cdot {l_{COM}}^2 = (4.6) * (0.249^2) = 0.2852 kg \cdot m^2$$

And then, for the torque, we just multiply by the joint acceleration,

$$T_{K,A} = I_{K,A} \cdot \dot{\omega}_K$$

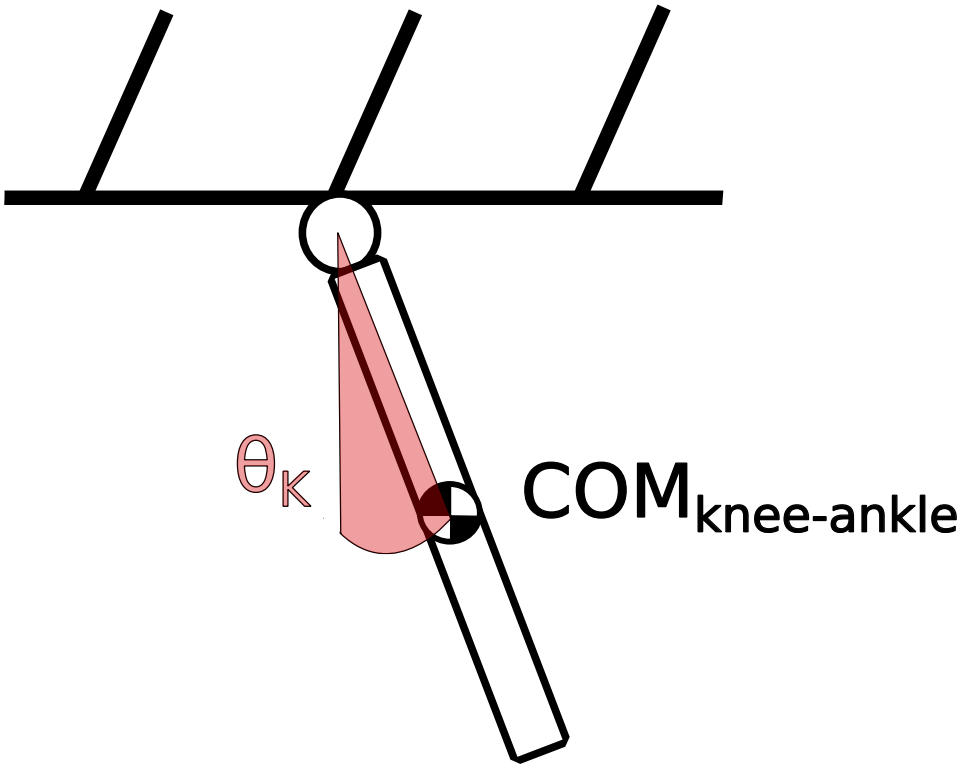

Figure 2.24: Simple pendulum scheme where θ_K is the knee angle

Then, for the gravity component:

$$T_{gravity} = (M_{foot} + Mprosthesis) \cdot g \cdot l_{COM} \cdot \sin\theta_K$$

Summing the two torques together (have to pay attention to the sign of the torques since when the leg is flexed the gravity goes against the muscle action, while, when the leg is swung, the gravity component helps us)

$$T_{tot} = T_{K,A} + T_{gravity}$$

Results The tibial component on the whole torque value and the foot component where further evaluated to understand which one would have more influence. The results show that, by considering a simple pendulum model, the foot inertia is about 10 times less than the knee inertia

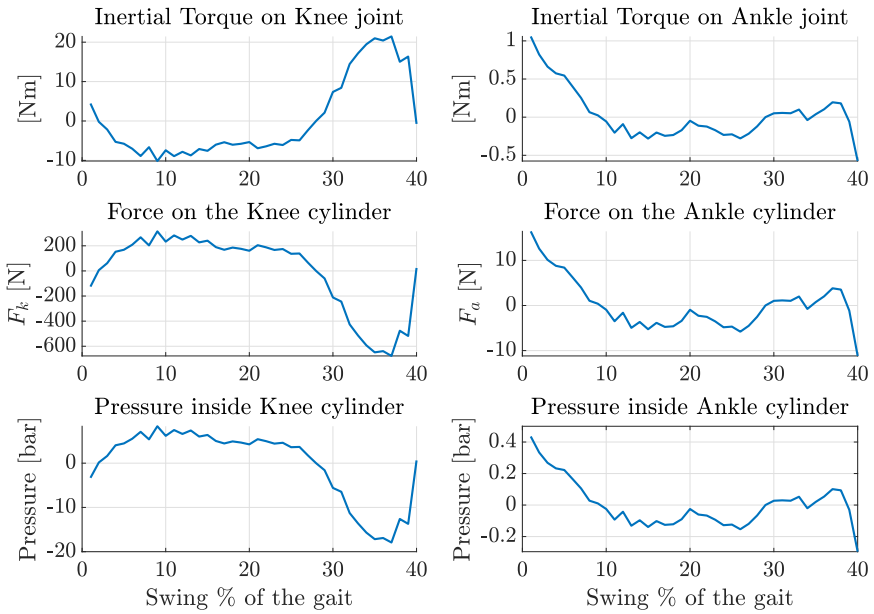

Figure 2.25: Various data form simple pendulum assumption

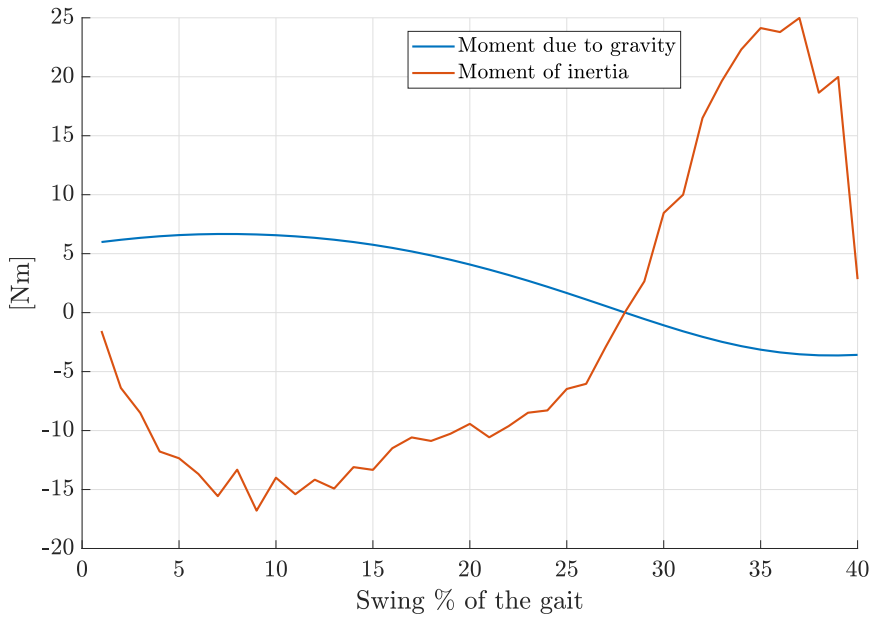

Figure 2.26: Moments due to inertia and gravity

Double pendulum assumption

The swinging motion of the leg can be much better represented with a double pendulum modelling (a triple pendulum would be even better); however it is more complex.
In Fig. 2.27 a representation of the double pendulum model.

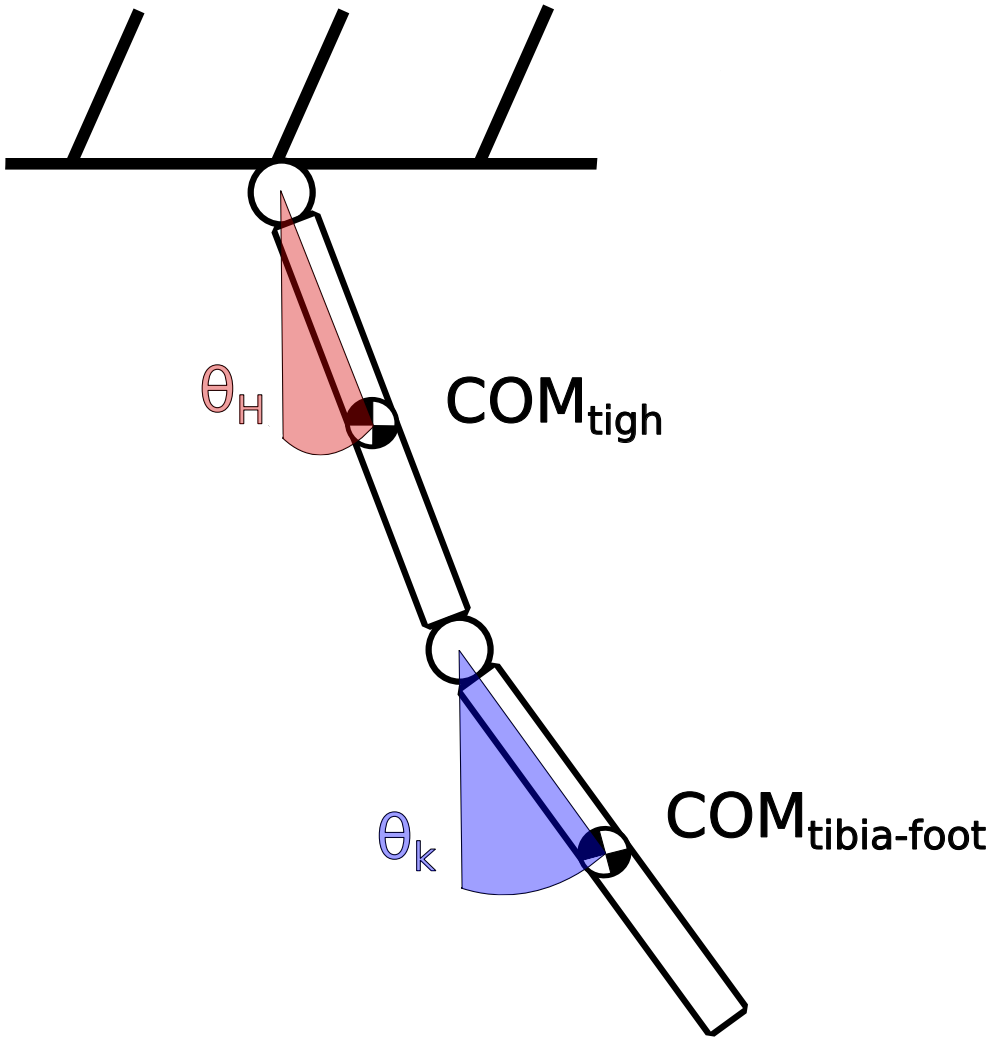

Figure 2.27: Double pendulum scheme where θ_H is the hip angle, while θ_K is the knee angle

Note that for the calculations, a double compound pendulum was considered as inertia parameters can be easily obtained from the tables of [31].

Calculations First of all, we define the lengths, weights and inertiae of the single components: we consider the thigh element as having the same weight of the physiological one for a standard subject, while the tibia-foot component is approximated by the estimation of the weight of the prosthesis.

- Tigh:
  - $M_{tigh} = 7.85$ kg
  - $\rho_{gyration} = 13.85$ cm
  - x = distance from hip of the COM = 18.57 cm

  $J_1 = I_{tigh} = M_{tigh} \cdot {\rho_{gyration}}^2 + Mtigh \cdot x^2 = 0.4217kg \cdot m^2$

- Prosthesis:
  - $M_{prosthesis} = 4$ kg
  - $\rho_{gyration} = 20.8$ cm
  - x = distance from knee joint of the COM = 30.23 cm

  $J_2 = I_{prosthesis} = M_{prosthesis} \cdot {\rho_{gyration}}^2 + M_{prosthesis} \cdot x^2 = 0.54kg \cdot m^2$

We utilize the Lagrangian approach to tackle this problem, our objective is to find two lagrangian equations that describe the movement of the two components (tigh and tibia-foot).

Location of the centers of mass

$$\begin{pmatrix} x \\ y \end{pmatrix} = \begin{pmatrix} 0.43 \cdot l_1 \cdot \sin\theta_H & l_1 \cdot \sin\theta_H - 0.5 \cdot l_2 \cdot \sin\theta_K \\ -0.43 \cdot l_1 \cdot \cos\theta_H & -l_1 \cdot \cos\theta_H - 0.5 \cdot l_2 \cdot \cos\theta_K \end{pmatrix}$$

Derivate to compute the velocities

$$\begin{pmatrix} \dot{x} \\ \dot{y} \end{pmatrix} = \begin{pmatrix} 0.43 \cdot l_1 \cdot \cos\theta_H \cdot \dot{\theta}_H & l_1 \cdot \cos\theta_H \cdot \dot{\theta}_H - 0.5 \cdot l_2 \cdot \cos\theta_K \cdot \dot{\theta}_K \\ 0.43 \cdot l_1 \cdot \sin\theta_H \cdot \dot{\theta}_H & l_1 \cdot \sin\theta_H \cdot \dot{\theta}_H + 0.5 \cdot l_2 \cdot \sin\theta_K \cdot \dot{\theta}_K \end{pmatrix}$$

Kinetic energy

$$T = \frac{1}{2} \cdot (m_1 \cdot ({\dot{x_1}}^2 + {\dot{y_1}}^2) + m_2 \cdot ({\dot{x_2}}^2 + {\dot{y_2}}^2) + J_1 \cdot \dot{\theta}_H^2 + J_2 \cdot \dot{\theta}_K^2)$$

and substituting translates into:

$$T = \frac{1}{2} \cdot (J_a \cdot \dot{\theta}_H^2 + J_b \cdot \dot{\theta}_K^2 + J_x \cdot \dot{\theta}_H \cdot \dot{\theta}_K \cdot \cos(\theta_H + \theta_K))$$

where

- $J_a = 0.185 \cdot m_1 \cdot {l_1}^2 + m_2 \cdot {l_1}^2 + J_1$
- $J_b = 0.25 \cdot m_2 \cdot {l_2}^2 + J_2$
- $J_x = m_2 \cdot l_1 \cdot l_2$

Potential energy

$$V = m_1 \cdot g \cdot y_1 + m_2 \cdot g \cdot y_2$$

and substituting translates into:

$$V = -\mu_1 \cdot \cos\theta_H - \mu_2 \cdot \cos\theta_K$$

where

- $\mu_1 = 0.43 \cdot m_1 \cdot g \cdot l_1 + m_2 \cdot g \cdot l_1$
- $\mu_2 = 0.5 \cdot l_2 \cdot g \cdot m_2$

Lagrangian equation

$$\mathcal{L} = T - V$$

$$\frac{d}{dt}\frac{\partial \mathcal{L}_t}{\partial \dot{q}_i} = \frac{\partial \mathcal{L}_t}{\partial q_i}$$

$$\downarrow$$

1. $$J_a \cdot \ddot{\theta}_H - J_x \cdot \ddot{\theta}_K \cdot \cos\theta_H + \theta_K + J_x \cdot \dot{\theta_K}^2 \cdot \sin\theta_H + \theta_K + \mu_1 \cdot \sin\theta_H = M_{hip}$$

2. $$J_b \cdot \ddot{\theta}_K - J_x \cdot \ddot{\theta}_H \cdot \cos\theta_H + \theta_K + J_x \cdot \dot{\theta_H}^2 \cdot \sin\theta_H + \theta_K + \mu_2 \cdot \sin\theta_K = 0$$

And these are finally our Lagrange equations which describe the motion of the double pendulum. The first equation equals the hip momentum M_{hip} as that is the only external torque that we keep into consideration (no losses assumed).

2.8.2 Motor choice

Knowing the magnitude of the inertiae into play we can determine the amount of torque that our motor should provide. To understand this, we can just translate the torque at the knee into torque at the motor keeping into account the components efficiencies.
First of all, we calculate the torque required at pump level:

$$\boldsymbol{T_{pump} = D_m \cdot \Delta p}$$

And, considering the two cylinders in parallel, $Ap_{eq} = 2A_K$, equivalent area of parallel cylinders

$$T_{pump} = D_m \cdot \frac{(F_A + F_K)}{Ap_{eq}} \cdot \frac{1}{2 \cdot \pi \cdot \eta_{pump}}$$

Note: F_A and F_K were taken from the inertia calculations forces.
This can be then translated into motor torque by factoring in the efficiency

$$\boldsymbol{T_{motor} = \frac{T_{pump}}{\eta_{motor}}}$$

This yields a curve representing the motor torque that we would have to provide if we chose to actively power the whole swing phase.It can then be smoothed out:

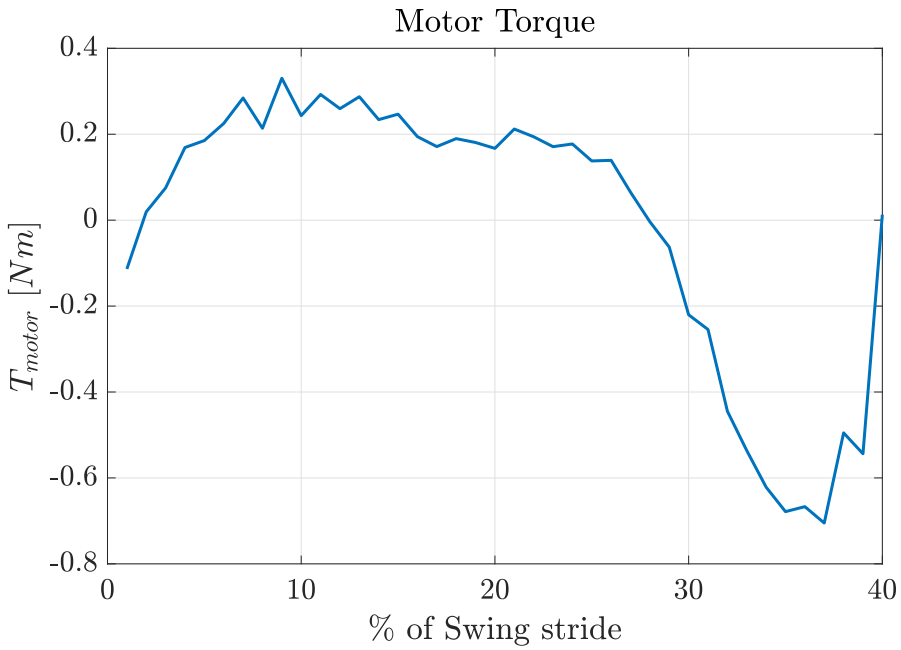

Figure 2.28: Non-smooth motor torque during swing phase

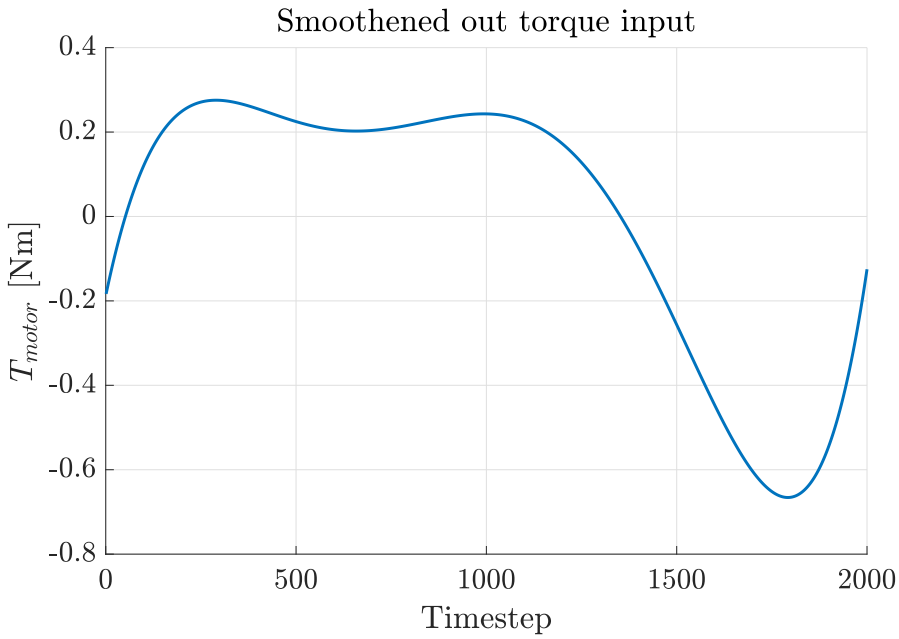

Figure 2.29: Smoothed out motor torque during swing phase

This leads us to the choice of a motor whose maximum torque has to be around 1 Nm. For such a requirement (and keeping in mind the speed of 3600rpm) the ILM 50x08 motor from TQ Robodrive was chosen [30].
This motor was deemed satisfactory for the initial theoretical requirements and it would be validated in the simulation phase.

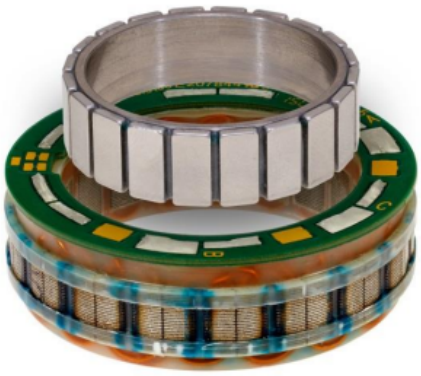

Figure 2.30: Image of the ILM50x08 by TQ Robodrive [30]

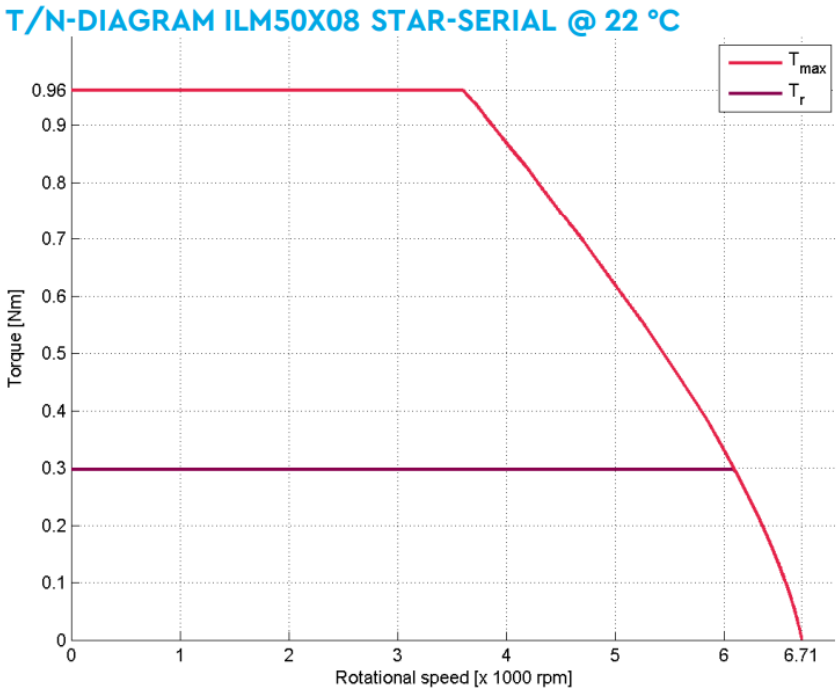

Figure 2.31: ILM50x08 Torque-Speed graph: the 0.3 torque line represents the rated torque, under which the motor works better with less Joule losses [30]

This motor presents the following characteristics *Note*: the star-serial configuration was chosen.

Possible improvements for the motor For this initial study on this prosthesis, a commercial motor was chosen, however, a custom design of the motor could be carried out, optimizing geometries and efficiencies of the working points.

Chapter 3

Results: Simulink and multibody simulation

Following the theoretical analysis, validation of the results is due. This was done through the MATLAB Simulink® environment, particularly with the help of the Simscape™ physical modelling environment.

Moreover, we want to be able to verify our capacity of controlling the leg during the swing phase, mainly by the use of a simple open loop custom control. This chapter is divided in the following sections:

- **Verification of the theoretical results**
- **Open loop control**

3.1 Verification of the theoretical results

We want to verify the theoretical results in Simscape™ and see if our assumptions lead to the expected results and whether said results are realistic and compatible with an efficient prosthesis design.

3.1.1 Fixed-displacement pump

- **efficiency**: We chose to model the pump with a one-point general efficiency, as, to have a complete efficiency map, an in-depth characterization would be needed and this is not in the scope of this thesis.
- **fluid viscosity**: as transmission fluid ATF Dexron III was chosen.

- **no-load torque**: this value specifies how much resistance the pump opposes when no load is attached to it. It is a hard value to characterize, so a low value was chosen to influence the model towards the ideal side.

Table 3.1: Fixed-Displacement pump values

Displacement	2.05 $[cm^3/rev]$	Volumetric efficiency at nominal conditions	0.75
Nominal shaft angular velocity	3600 [rpm]	No load torque	0.01 $[N \cdot m]$
Nominal pressure gain	10 [bar]	Friction torque vs pressure gain	1e-6 $[N \cdot m/bar]$

3.1.2 Electric motor

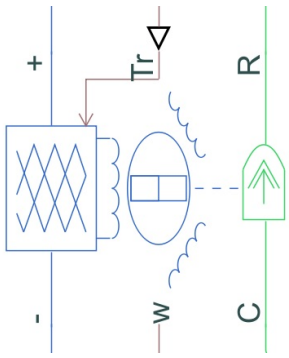

Figure 3.1: Electric motor block

The Electric motor was modelled with a block from the Simulink library. This motor model has a 1-point efficiency, which was assumed to be enough in this situation, since a more extensive modelling could be a long work outside the scopes of this thesis.

The block has the following inputs and outputs:

- **Battery voltage**, *input* : 48 Volts, from datasheet
- **Reference torque**, *input* : torque reference signal that the motor will try to follow with its embedded controller
- **Motor speed**, *output*

Table 3.2: Electric motor parameters

Maximum torque	0.96 $[N \cdot m]$	Motor efficiency	0.8
Maximum power	210 [W]	Speed at which efficiency is measured	3600 [rpm]
Torque control time constant	1 $[\mu s]$	Torque at which efficiency is measured	0.3 $[N \cdot m]$

- **Motor mechanical ports**: Mechanical rotational ground (C) and rotor shaft port (R) which are then connected to the mechanical ground and the pump shaft respectively.

3.1.3 Hydraulic cylinders

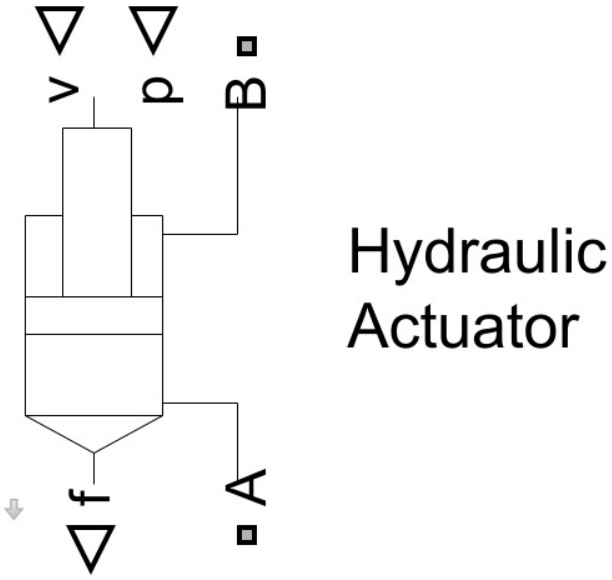

Figure 3.2: Hydraulic actuator block

This block comes from the "Simscape Multibody Multiphysics Library" [32] and permits the characterization of a double-acting cylinder with hardstops. Moreover, it allows the input of position and velocity of the piston and to output the force, permitting an open loop control of the model.
The main parameters are:

- **Piston Area**: A_p

- **Cylinder stroke**: describes the range of motion that the piston has inside the cylinder
- **Hardstop properties**
  - Stiffness → high value since to achieve a rigid hardstop
  - Damping
- **Friction properties**
  - Breakaway Force
  - Breakaway Velocity
  - Coulomb Friction Force
  - Viscous Friction Coefficient

  note that these last 4 properties are hard to determine since it is generally not easy to describe friction coefficients without setting up ad-hoc experiments. Consequently, low values were assigned to these parameters so that they are close to ideal.

3.1.4 Valves

Hydraulic bi-directional valves are the means of regulation of flow in the cylinders and consequently the movement of the leg. Simulation-wise, a variable orifice model was used.

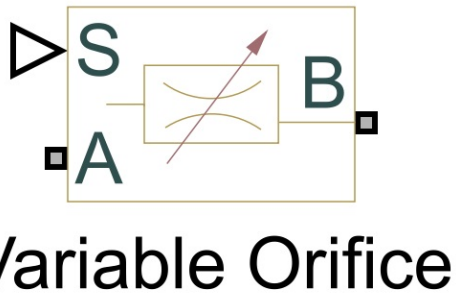

Figure 3.3: Variable orifice block

The block was then implemented in the following Simulink circuit to verify its functioning

The valve is defined by pressure-flow characteristic (three parameters):

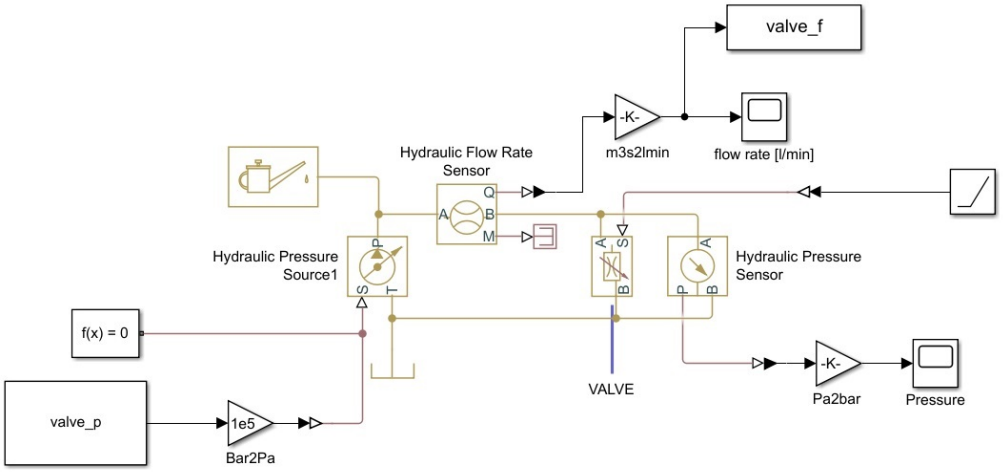

Figure 3.4: Simulink circuit for the valve characterization: a pressure input is given to the circuit and the closing of the valve is changed via a ramp block according to the simulation time

- **Orifice opening vector** θ
- **Pressure differential vector** d_p
- **Volumetric flow rate table** $q(\theta, dp)$

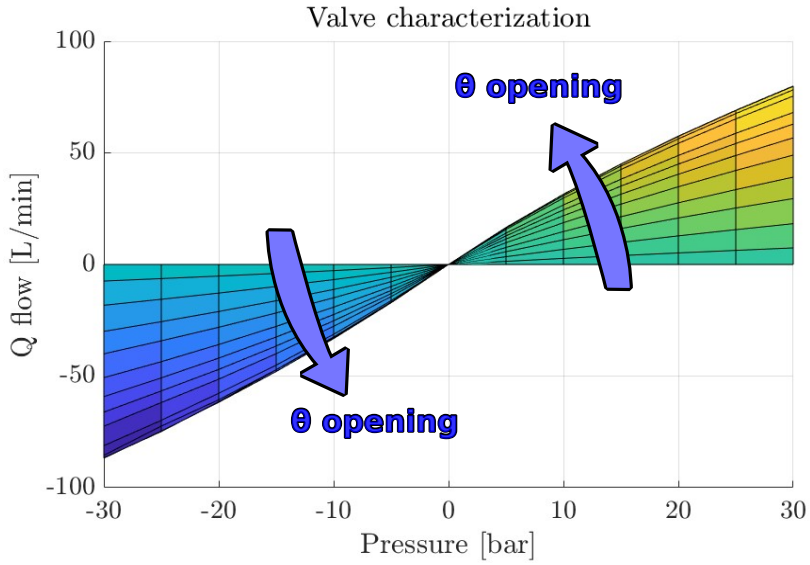

Figure 3.5: Variable characterization, by closing the valve the flow diminishes even if the pressure remains unchanged. This graph is a result of the 3.4 simulation

The main parameters describe the following characterization, which correlates the pressure-flow graph to the orifice opening. The remaining flow with a shut valve results in $9.8 \cdot 10^{-3} L/min$

3.2 Verification of the flow sum

Having a good understanding of the components of the circuit allows us to have a good degree of confidence in the complex models that we can create.
The first verification needed pertains the flow sum at the upper node of the hydraulic circuit. We want to make sure that theoretical results and simulation results coincide or differ very slightly due to the higher degree of realism characteristic of the Simulink parametrization of the components.
The following Simscape model was built to verify this. A source of ideal linear velocity is inputted in the cylinders block. The velocities are calculated from the derivative of the angular positions and transformed into linear velocities by knowing the lever arm during the whole stride 2.17. This, as the formula for flow in the cylinders is $Q_{cylinder} = v_{cylinder} \cdot A_p$, simulates the hydraulic flow in the circuit during the whole stride. Eventually, we measure the flow at the upper node of the circuit and transform it into the proper unit (L/min). Afterwards we can

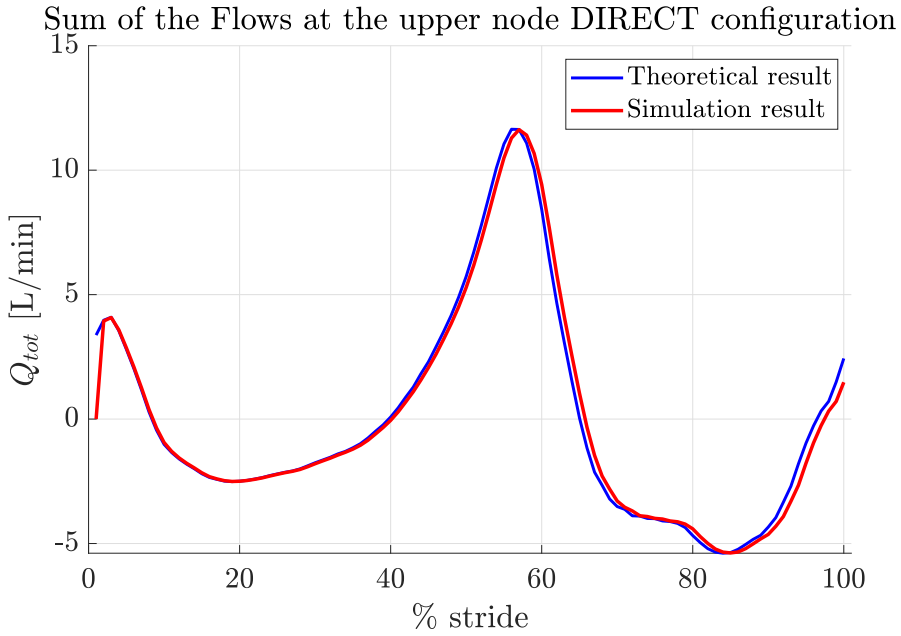

Figure 3.6: Comparison between theoretical sum result and simulation result

compare the simulation result with the theoretical one and verify that the two flow

sums are indeed equal and confirm the result of the $Q_{tot} = sign(v_{cylinder_K}) \cdot |Q_K| - sign(v_{cylinder_A}) \cdot |Q_A|$ equation, as seen in and Fig. 3.6.

3.3 Multibody model

As the Mathworks® website states about Simscape Multibody :"Simscape Multibody™ (formerly SimMechanics™) provides a multibody simulation environment for 3D mechanical systems" [33].
This environment was used to model the leg prosthesis physically so that simulations can be extended also to physical objects and the effect of forces, inertiae and motion can be seen in a practical way.
Components can be modelled directly in the multibody environment or can be imported from a design software. In my case, the parts were first designed in SOLIDWORKS® and then exported to Simulink (apart from the cylinders, modelled directly in the Multibody environment).

- **Thigh**
- **Tibia**
- **Foot**
- **2 Hydraulic cylinders** (modelled as two passing cylinders)

I would like to emphasize that these components are merely an ideal representation of the prosthesis components, although, the proportions and geometries reflect the theoretical analysis carried out in chapter chapter 2.

To connect all the prosthesis components, frames of reference were assigned to particular points on each piece (e.g., joint rotation axes, attachment points). Subsequently, these frames of reference were connected to each other by means of joint blocks, thus making relative movement available between the various components.
A rotation between the components was modelled through a revolute joint, while a prismatic joint allowed to model the cylinders compenetration (relative movement between piston and chamber).
NOTE: All components were assigned the weights calculated from chapter 2.

Subsequently, inertiae were calculated automatically (given the mass of the object) by the software. It was assumed that these inertiae approximated well enough the real ones, or at most, they are conservative in that sense.

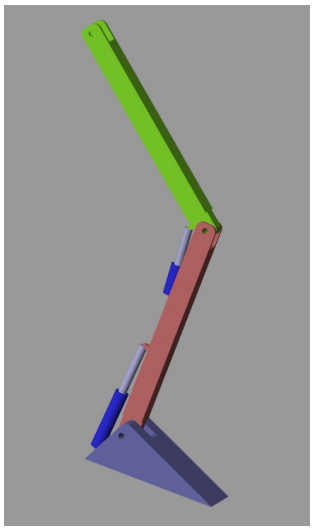

Figure 3.7: Assembled prosthesis in the Multibody™ environment.

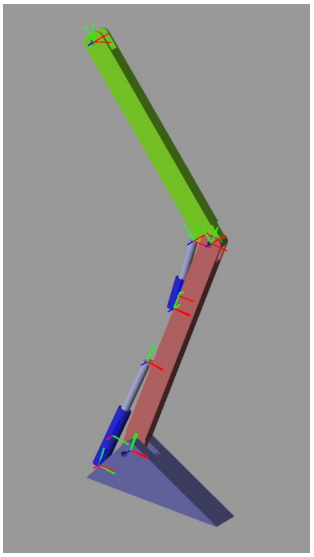

Figure 3.8: Assembled prosthesis with frames of reference

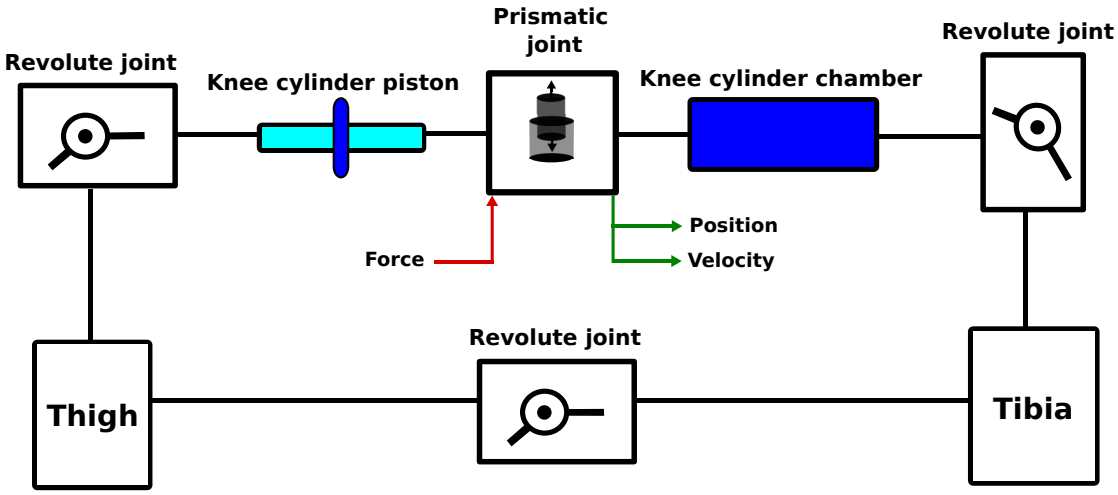

Figure 3.9: Multibody connection schematic

3.4 Swing modelling

As was discussed in chapter 2, it was chosen to model the leg components only during the "Swing phase".

Description This first model investigates the swinging motion without hip movement nor rotation. The motion is produced solely by gravity and forces acting

in the cylinders (which come from the motor activation), as there are no contacts with the ground. The thigh part is still and connected to the ground reference.

Control The control strategy utilized was an open-loop one, as we merely want to inquire in the capabilities of the motor to satisfy a certain requirement in cylinder actuation to model accurately the joints' trajectory during swing.
Velocity measurements coming from the prismatic joint block are fed as input to the Simscape hydraulic cylinder model. This, in return (through the use of virtual force and velocity sensors), calculates the force applied on itself and sends it back to the multibody block.

Results Thanks to a custom torque reference signal (achieved heuristically), it was possible to achieve a satisfactory trajectory of the leg, while maintaining motor power under the admitted values of 2.31.

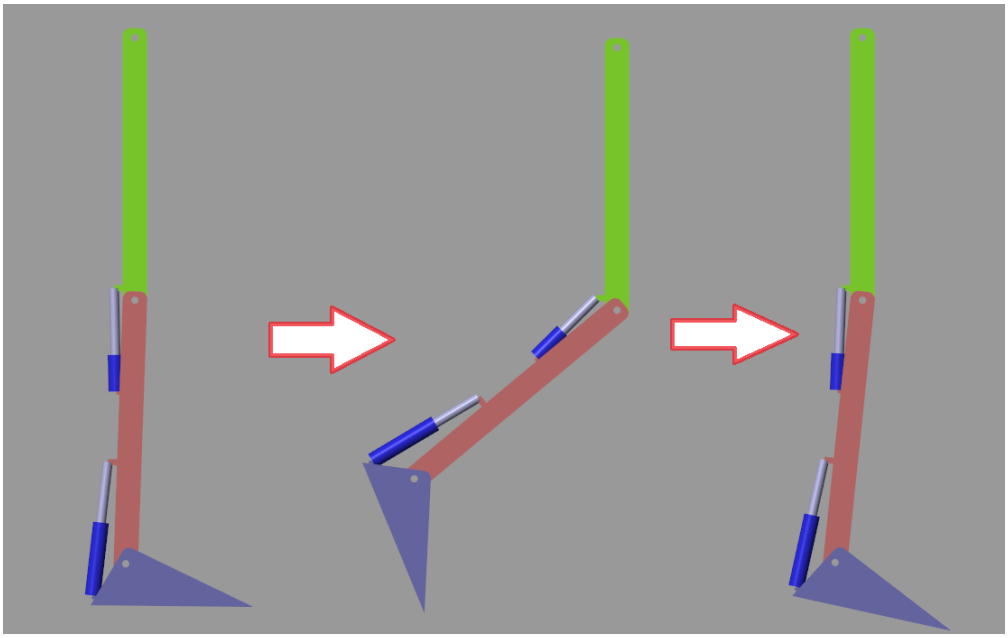

Figure 3.10: Temporal succession of movement for a swing phase with no hip movement

As can be seen, the performance is not optimal since there is a significant delay and error between simulated and physiological angles

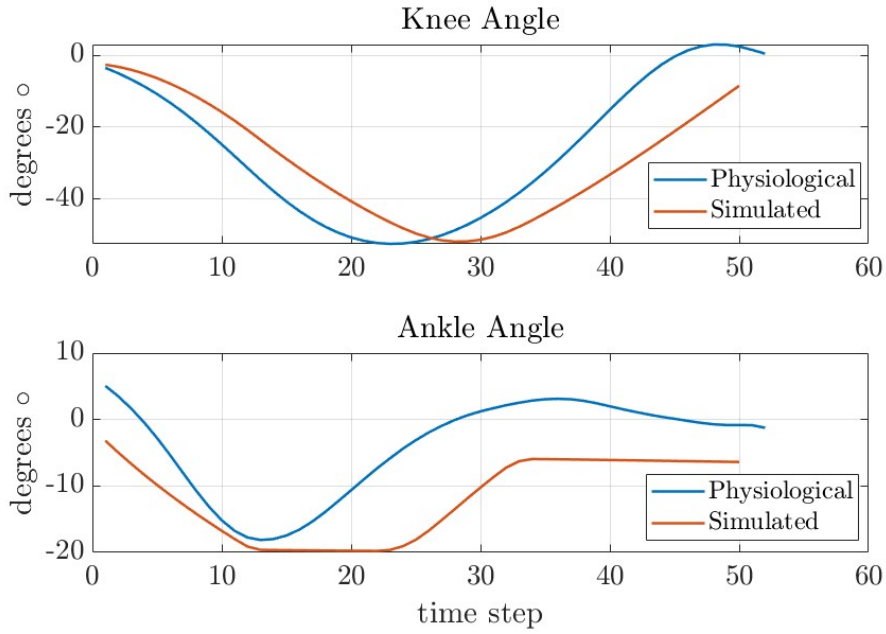

Figure 3.11: Comparison between physiological knee and ankle angles and simulated ones (no hip assistance)

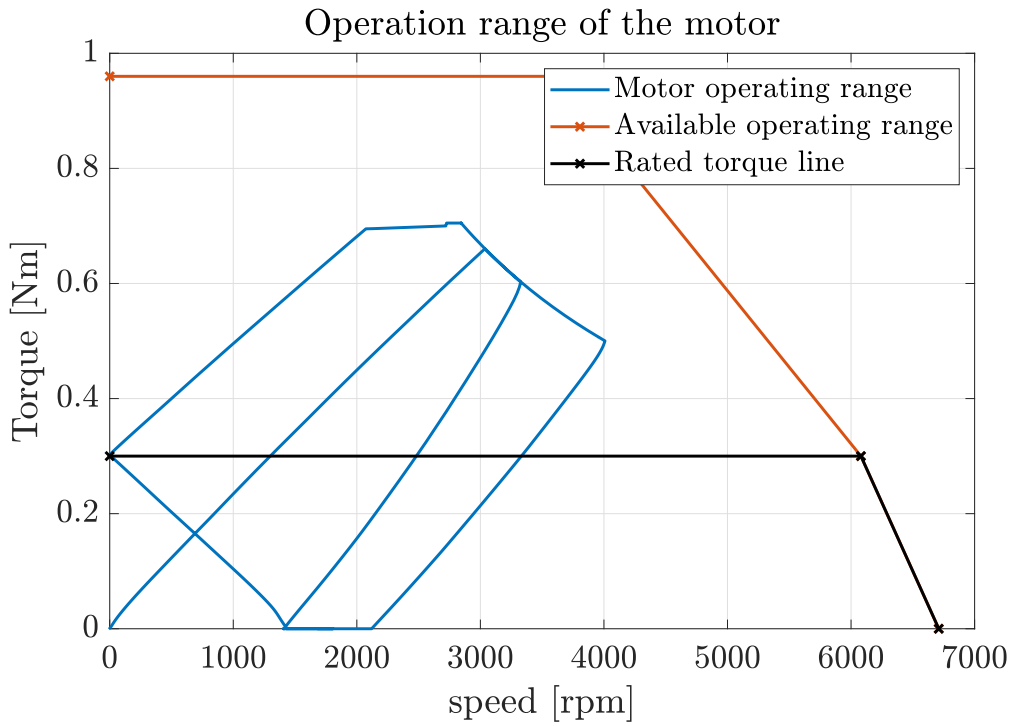

Figure 3.12: Motor operating range for a swing phase with no hip assistance

As can be seen in Fig. 3.12 the motor working range is well below the available operating range (from motor datasheet). This is acceptable, however it can be argued that, to lower the torque output, the working points could be moved toward higher velocities, so to have higher flows but lower torques. This is to bring the blue line closer to the rated torque line, under which the motor works at higher efficiencies and, most importantly, is less affected by Joule losses due to heating.

3.5 Swing modelling with hip movement

Description The simulation is similar to the one described above, nonetheless in this case the hip rotation movement is added. The hip angle was extrapolated from Lencioni's et. al dataset [21]. The hip movement helps significantly during the swing phase, as body inertia and thigh movement are the principal authors of motion of the shank and foot. We should expect a reduced motor effort.
Since we are simulating only for swing, the hip initial position corresponds to the moment when the leg detaches from the ground and the final position to when the foot touches the ground again 3.13.

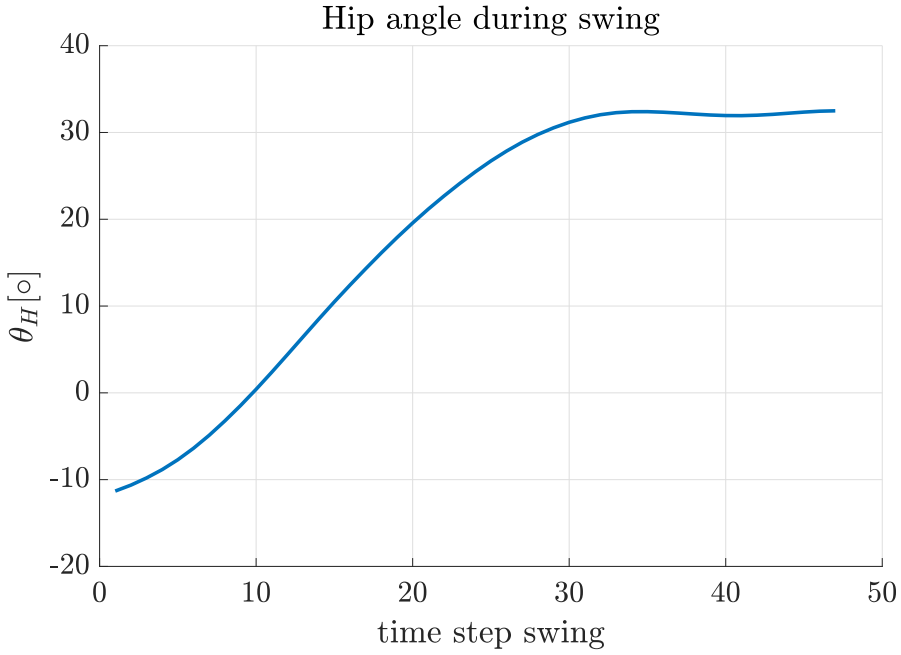

Figure 3.13: Hip angle during Swing phase

Control The control is open-loop as in the previous simulation.

Results The motor effort is reduced by about 50%, besting the previous performance. This can be seen by figure 3.14. Moreover, the operating range of the motor is completely under the rated torque line as in Fig. 3.15. This is ideal and also much closer to reality, in fact, passive prostheses that utilize the swing movement of the hip to propel the leg forward exist and are the most popular of their kind. Adding the motor action helps to swing the leg faster and, possibly, reduce muscle activation and imbalance in the hip due to compensation of the missing limb muscles.

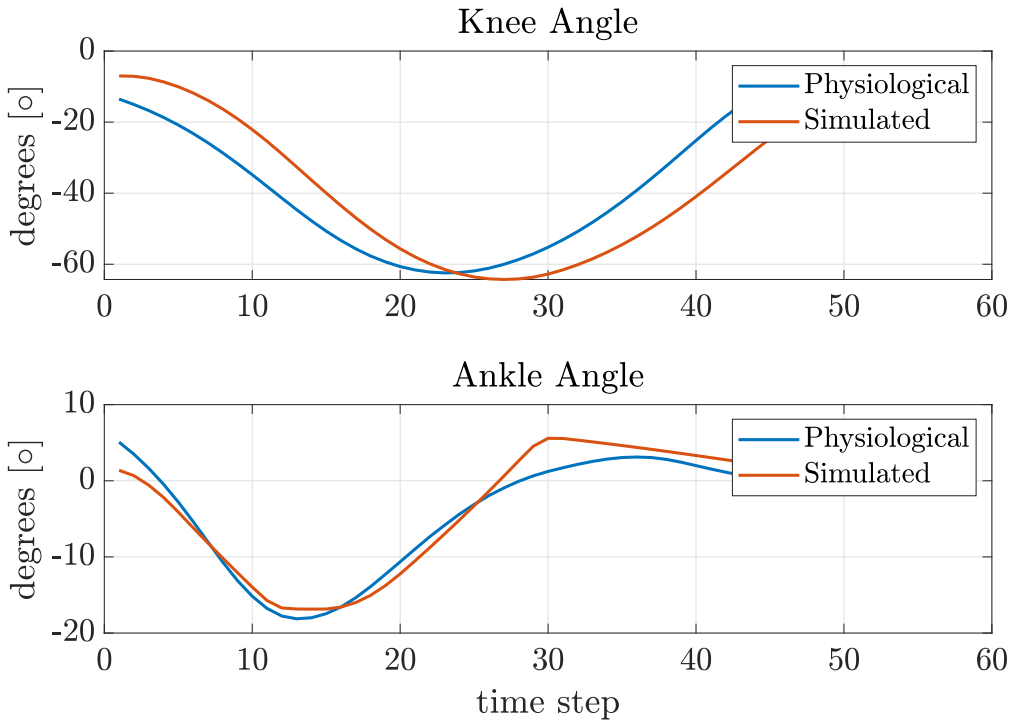

Figure 3.14: Comparison between physiological knee and ankle angles and simulated ones

- $RMSE_K = 10.3°$ (NO hip $RMSE_K = 13.6°$)
- $RMSE_A = 1.8°$ (NO hip $RMSE_A = 8.5°$)

Note: The RMSE of the knee is higher because the prosthesis is a bit late to follow the trajectory, however, the physiological trajectory is repeated accurately. This delay could be due to a slight insufficiency in the open loop control of the motor and valves.

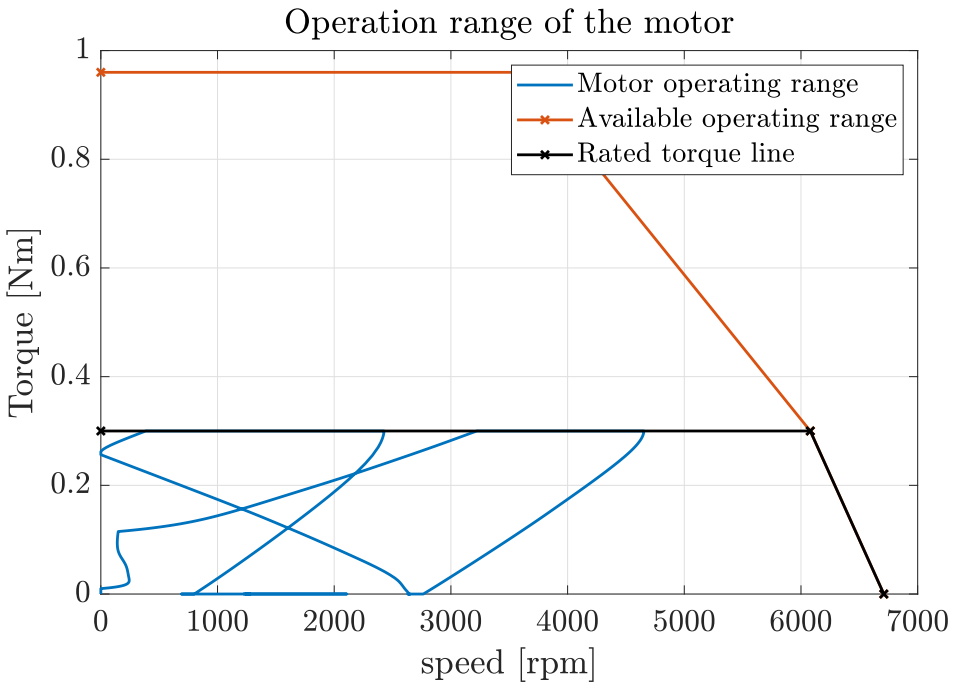

Figure 3.15: Motor working range during Swing

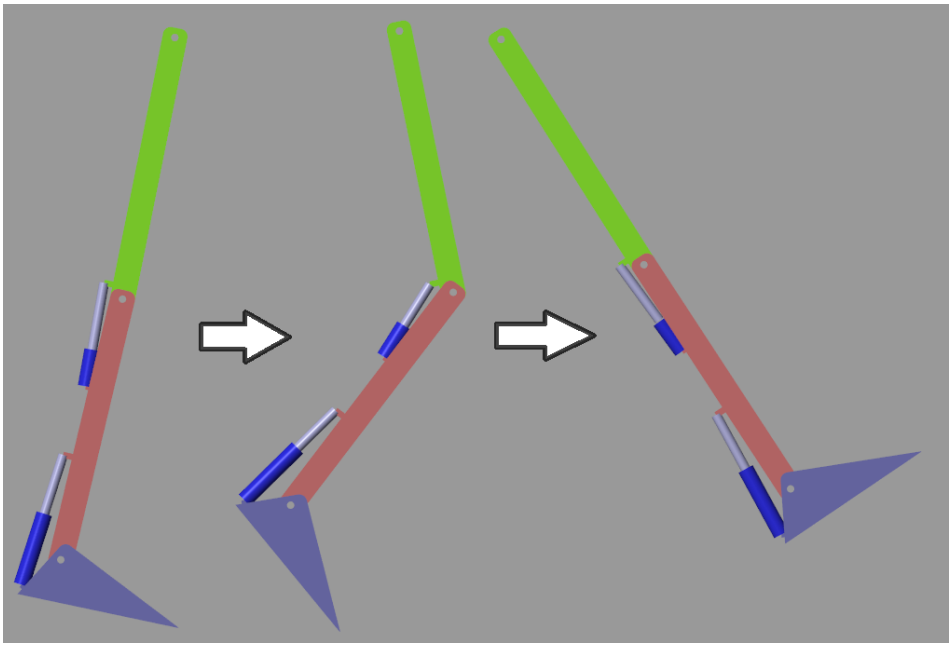

Figure 3.16: Swinging motion with hip movement

3.6 Stance modelling

After having characterized the Swing phase and understood the prosthesis components' behavior, the work focused on modelling the Stance phase as well.

Description This phase of the gait cycle is characterized by the contact with the ground, which produces high forces since all the weight of the body is shifted onto the leg and forward, in a controlled falling motion. The ground is modelled in Simulink by a plane, which, connected to the world reference frame, comes into contact with the foot of the prosthesis previously modelled. The motion of the body is simulated by a trajectory imposed to the hip joint.

3.6.1 Contact modelling

The actual contact is modelled by a Simulink block which simulates various parameters of the contact. The following values were estimated:

- **Stiffness of the contact**: $\frac{\text{Weight on contact}}{\text{displacement of the interface}} = k = 780/0.01$ [N/m]
- **Critical damping**: $\beta_{cr} = 2 \cdot \sqrt{k \cdot m} = 4949$ $[kg/s]$
- **Damping of the contact**: $\beta = 7800$ [N/(m/s)] 10 times less than the stiffness
- **Damping ratio**: $\frac{\beta}{\beta_{cr}} = 1.57$
- **Static friction coefficient**: $\mu_s = 0.85$
- **Dynamic friction coefficient**: $\mu_d = 0.75$

  These 2 last values represent the friction coefficients of the *asphalt-rubber* interface.

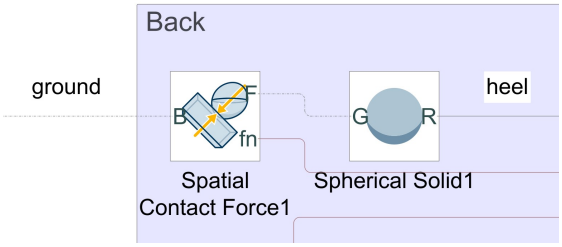

Figure 3.17: Contact blocks

3.6.2 Hip stiffness modelling

By simulating the model, I came across an interesting problem: the forces measured on the cylinders were of orders of magnitude higher that the ones that I had expected. Although it might not be the only reason for this, rigidity of the model was deemed responsible for such high forces, since there is no damping nor stiffness modelled between hip and ground.
This makes the model ideally rigid but far from reality. In fact, for a transfemoral amputee, the femoral stump is present with the remaining muscles to dampen the forces on the knee. Moreover, the hip muscles and joint articulation (cartilage and sinovial fluid) make up for a good dampening of the motion.
Unfortunately, it is very difficult to characterize stiffness and especially damping of anatomical parts since, taking the muscles as example, these vary in length non-linearly and so have non-constant and non-linear values of stiffness and damping that depend on the position, angle and applied force on the joint (or bone or muscle).
To overcome this problem, I tried to model a spring-damper system attached to the hip revolute joint. This was done by simply modelling two compenetrating cylinders that behaved like a spring-damper.
Modelling such spring-damper parameters is complex, difficult and prone to errors. The hip model I propose for the simulation is an equivalent model that allows to simulate the behavior of the leg without having to identify such parameters.

3.6.3 Hip movement modelling

The hardest problem to overcome in the modelling of a 1-legged stride simulation model is to determine how the whole body moves the leg, as the inertia of the leg is small compared to the one of the whole body. In simple words, it is necessary to determine a trajectory for the hip to follow, such that the Stance phase - Swing phase sequence is effected to a good degree of accuracy.

Why is this problem hard? There is a great degree of complexity in simulating the body motion. Moreover, the contact with the ground is dynamic, so accurate modelling becomes hard without precise measurements.

Control The hip joint was modelled by a cartesian joint + revolute joint (the cartesian joint allows for the movement in the X and Y direction while the revolute joint allows the rotation about the hip axis) as in Fig. **??**. The X and Y trajectory was taken from a dataset found in the Winter book [31] while the rotation angle come from Lencioni's dataset [21].

Two main problems emerged from this dataset and its application:

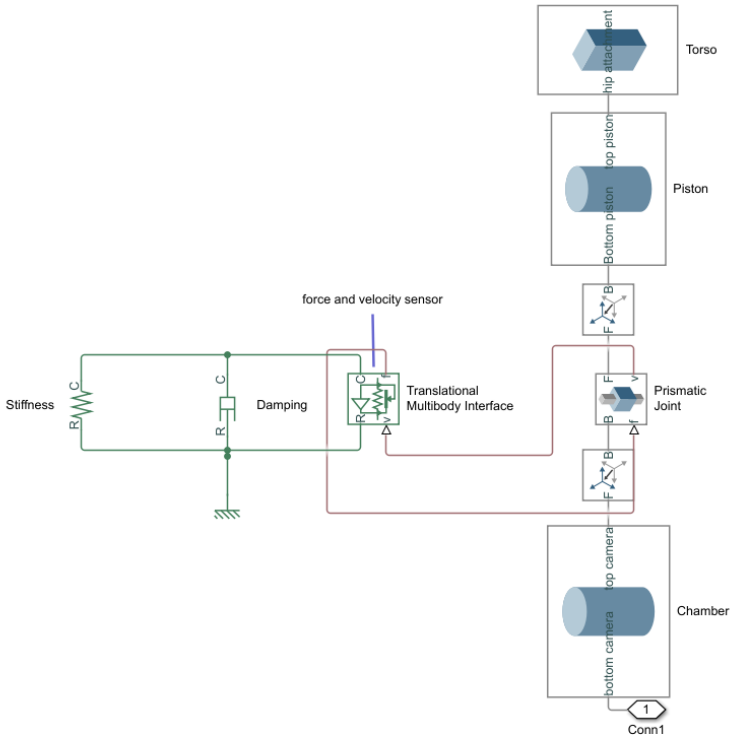

Figure 3.18: Hip stiffness and damping model

- **Datasets not corresponding to same subject**: As the datasets addressed two different subjects, trajectories had to be modified to resize the XY trajectory (which was taken from a light individual) to fit the displacements that the θ_{hip} would induce. Such task was not easy as every individual walks differently and each millimeter is important in this case. This problem was partially solved also thanks to the next point.

- **Imposing trajectories leads to force problems**: After determining the trajectories for the hip to follow, we can impose them in the joints. This however leads to very high forces on the leg, since imposing a trajectory means that a joint will impose a movement no matter the resistance it encounters. Instead, we would like our joint to follow "more or less" the given trajectory, so that the movement adapts to the forces on the ground.

  This was done by imposing a torque in each joint, controlled by a closed loop impedance controller. The controller's input is the trajectory error (between actual trajectory and measured one).

  The controller is of the form:

$$F = k \cdot error_{joint} - \nu \cdot v_{joint}$$

and the parameters k and ν are calculated heuristically. Especially, for the Y trajectory, the parameters are more stringent during the Swing phase, while slacker during the Stance phase.

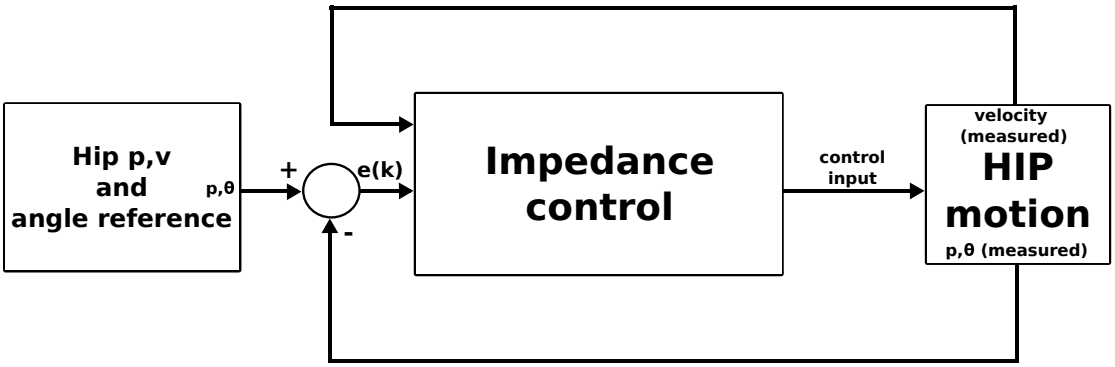

Figure 3.19: Impedance control scheme

Results The results of the control (over one whole stride) is the following one:

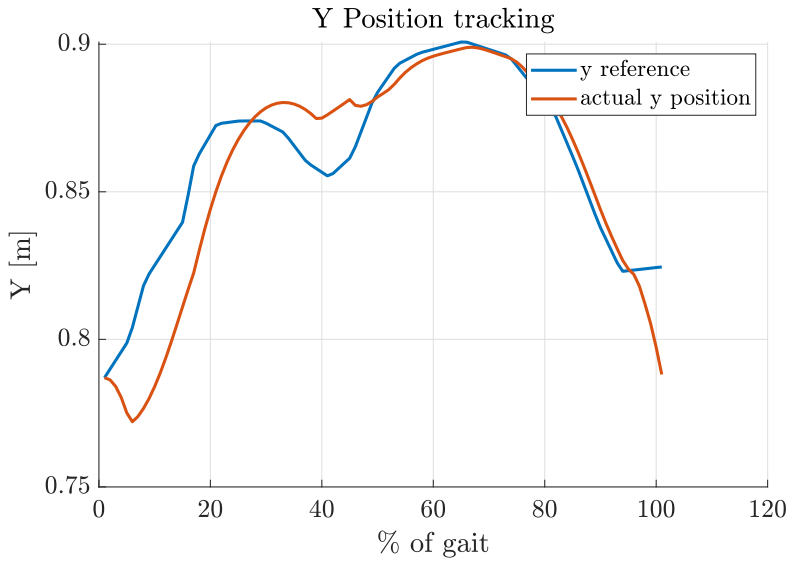

Figure 3.20: Tracked hip Y trajectory by the impedance control, note that during the stance phases it is much more slack

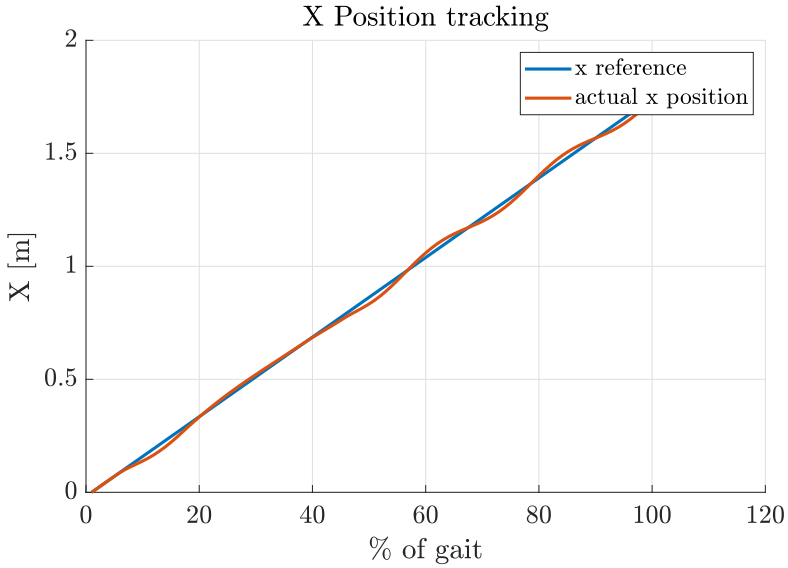

Figure 3.21: The X trajectory is followed closely to keep a constant walk velocity

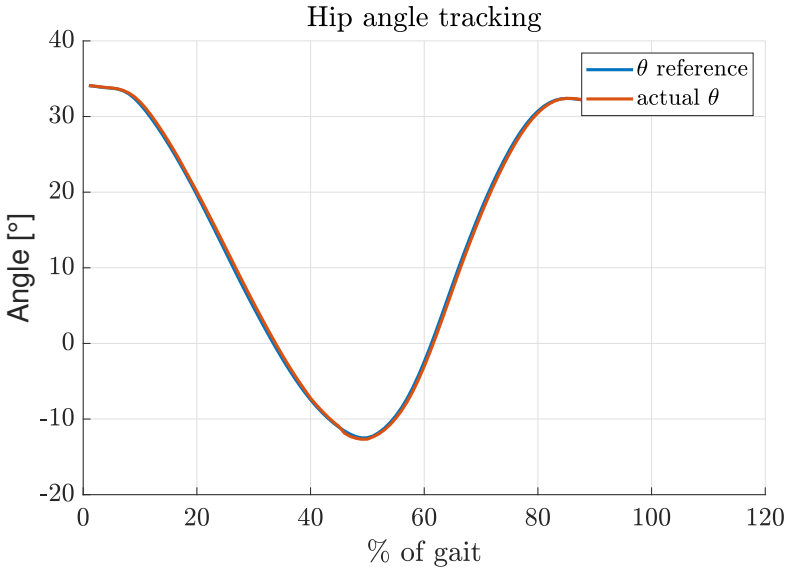

Figure 3.22: The θ_H trajectory is followed closely

3.6.4 Valves control

A simple state machine was built to determine which phase of the gait cycle the prosthesis is in, depending on sensor data.
Virtual contact sensors on the bottom of the foot send back the output to the state machine and this allows for the valves control. This sequence of states and

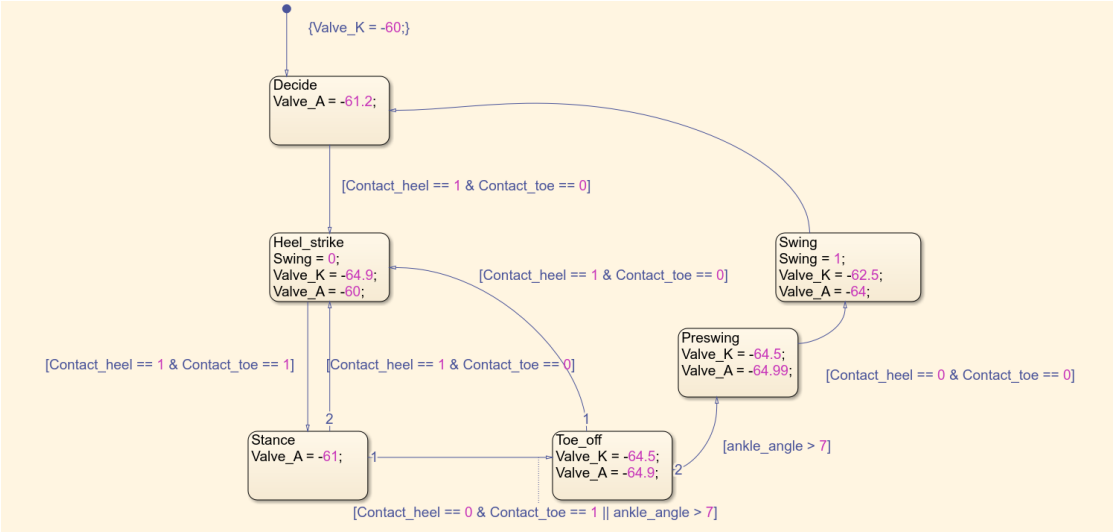

Figure 3.23: State machine with conditions and valves closing values

consequent closure of valves leads to the following result in 3.24: The knee and

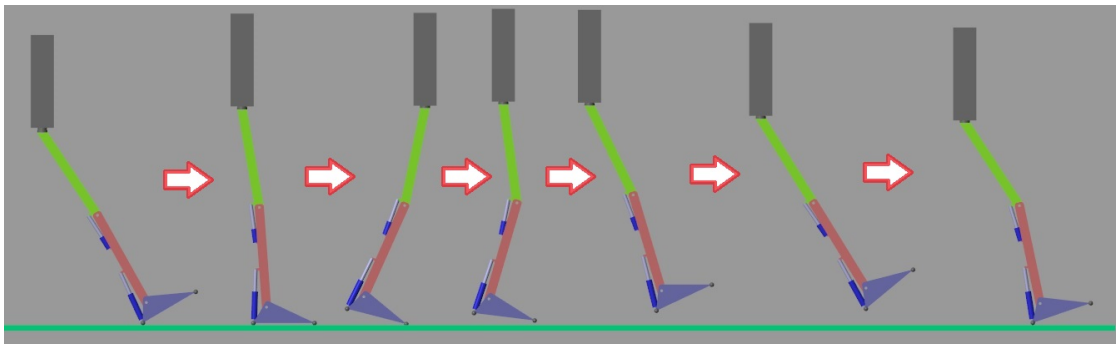

Figure 3.24: Whole stride sequence

ankle act completely passively, their movement being powered by the thigh swing and valve modulation.

3.6.5 Passive stride: results analysis

A passive stride (and so the typical transfemoral amputee stride) has peculiar characteristics:

- **Knee**
  - **Stance**: During stance, the knee is blocked in position by the valve, as

there is no positive power input to allow for a flexion followed by an extension (as it is in the physiological walk).

- **Swing**: The valves can be closed accordingly to the amount of displacement that we want to reach, so, ideally, we can have identical trajectories.

- **Ankle**:
  - **Stance**: Since we lack an elastic foot during simulation, the foot fits the ground contact shape. This makes for a much higher excursion for the ankle than the physiological one.
  - **Swing**: During swing the ankle valve is mostly closed off so that, when the foot lands, we approach the ground with a good angle.

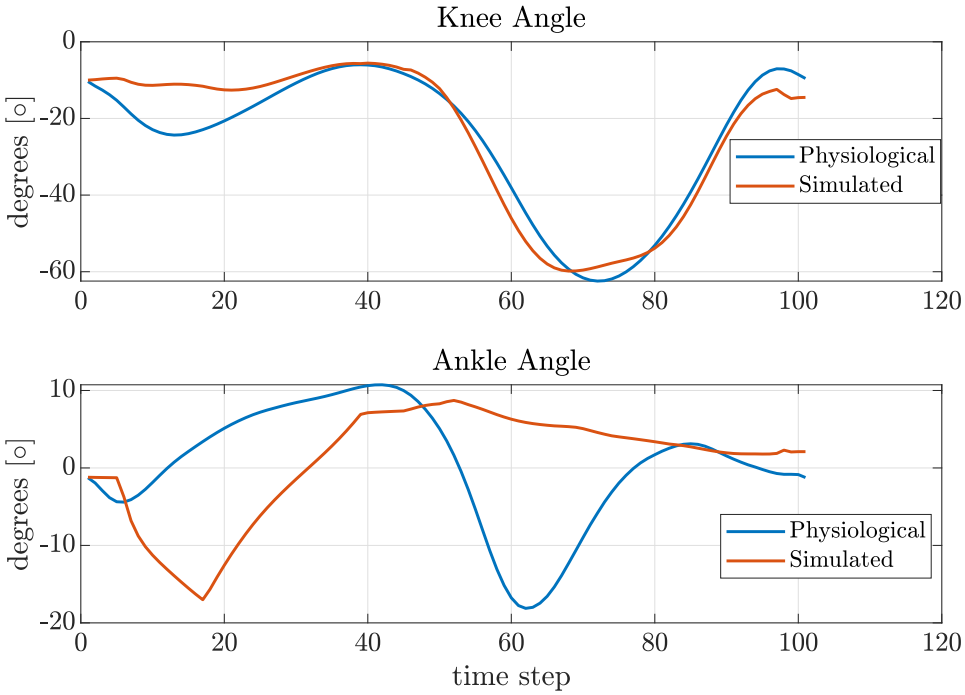

Figure 3.25: Angle differences during the whole stride

3.7 Alternative circuit configuration inquire

The circuit configuration used in the previous simulation is the direct configuration, as in 2.21. However, one more circuit configuration was considered for the prosthesis.

On the basis of the consideration that two cylinders in parallel push each other when a load is applied on either end, we inquired about the possibility of utilizing this effect to push the ankle cylinder during the braking action of the knee cylinder (e.g. during the "Stance" and "Toe-off" phases).

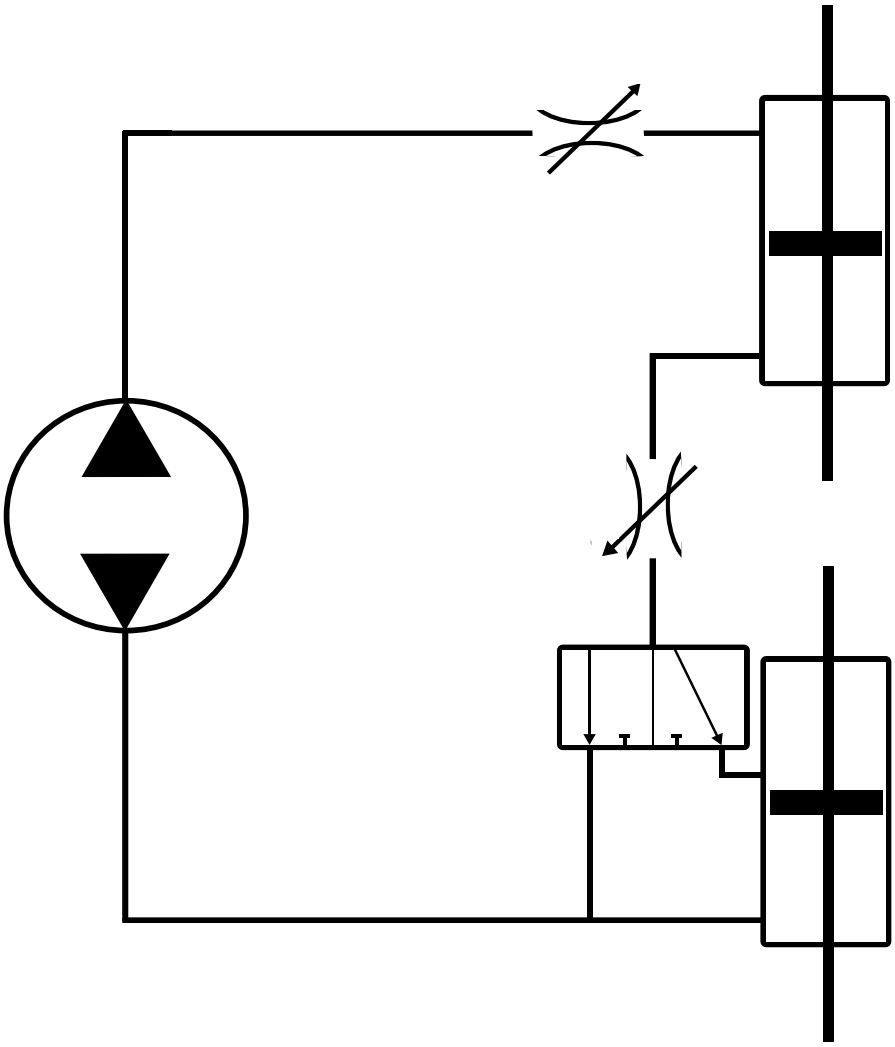

Figure 3.26: Alternative circuit configuration

Description The configuration in 3.26 includes 3 valves instead of 2 as in 2.21. This is its intended functioning during the different phases:

- **Stance**: Since the two cylinders are connected in series, we have that a load applied on one has an effect on the other cylinder as well. By shutting the hydraulic valve we get that the resistance seen by the pump is the one of the

knee cylinder (top) plus the one of the ankle cylinder (bottom), further adding the resistances of the valves. For example, if we load the knee cylinder and we open the variable orifice of the ankle, we get that the displacement of the knee cylinder will be the reproduced at the ankle cylinder (less efficiencies) since the piston areas are the same. Vice-versa we get that an extension of the ankle cylinder will lead to an extension of the knee cylinder.

This "Hydraulic redundancy" can be useful to brake the knee from bending during the stance phase since, by bending the ankle to go in "Toe-off position", we automatically have an extension of the ankle cylinder and so an extension of the knee cylinder, which pushed against the body weight force.

Moreover, if we assume that the knee bends slightly during the last moments of the stance, we have a flexion of the knee cylinder. This implies a flexion of the ankle cylinder and, so, a force that opposes the extension. It could be compared to the action of the Achille's tendon, which, by stretching during the dorsiflexion, becomes more tense and ready to spring back.

Such action was, wrongly, thought to be able to propel the ankle plantarflexion,or at least partially. However, this effect, is at most as large as the resisting force effect of a shut of valve on the cylinder ankle. In fact, the weight force on a closed cylinder, or, on a coupled ankle cylinder with the knee cylinder, will be basically the same.

- **Swing**: During swing, we have little need of rotating the ankle, so, we can decouple it from the knee by opening the VALVE and letting the pump see only the knee resistance. The performance is the same to the previously discussed swing phase simulation.

Results This configuration does not result in the desired effect. However, it could be useful for the "Hydraulic redundancy" principle in case the valves aren't able to close well during high loads. This effect could be applied also in case of very high loads during stance.

Chapter 4

Conclusions

The main objective of this thesis was to inquire in the possibility of realization of a multi-joint, under-actuated prosthesis for transfemoral amputees, and, if possible, to proceed in its preliminary sizing and analysis.
The prosthesis is of the semi-active type, so it actuates the leg only during certain phases of the walking cycle. Moreover, it actuates both knee and ankle through hydraulic cylinders, which are powered by an Electro Hydrostatic Actuation unit, which is comprised by an electric motor, a fixed-displacement pump (gerotor) and the hydraulic cylinders. Lastly, the hydraulic cylinders' movement is modulated by 2 hydraulics valves. The under-actuation approach allows to power both joints thanks to exclusively one actuation unit.
The proposed design was shown to be able to sustain and aid the gait cycle during all of its phases. The hydraulic circuit presented was effective in both actively powering the prosthesis (via the EHA unit) and passively braking thorough the high force phases of the gait cycle (e.g., "Stance phase") thanks to the control of hydraulic valves, effectively making the valve plus cylinder system function as an hydraulic damper. An existing dataset of physiological angles torques and powers for hip, knee and ankle joint was analysed and was the base for the theoretical calculations.
The geometries and positioning of the components were optimized for the patient's needs, specifically minimizing the knee cylinder lever arm to render the knee back-drivable ,and maximizing the ankle cylinder lever arm in order to reduce the forces on the latter.
Power requirements during the stride are different depending on which phase we look at. The "Stance phase" (which is the initial phase of the walking motion, where the foot is on the ground) is characterized by high forces on the leg since the weight of the body is entirely on it. The "Swing phase" instead (which is when the leg swings forward, the foot leaving the ground) is characterized by high velocities in the joints. By deciding to actively actuate the leg only during the "Swing phase", we

were able to lower the requirements on actuator power and dimensions. Such choice led to the conclusion of the theoretical analysis, from which emerged that it is possible to actuate the leg during the "Swing phase" while maintaining a reasonable size actuator with a motor of 1Nm of maximum torque and a fixed-displacement pump displacement value of 2.05 cm^3/rev. The "Stance phase" would be carried out through valve modulation and, in case, only partial assistance by the motor.
Such hypotheses were validated by simulations which were carried out in the Simulink environment. The simulations modelled, in a more realistic way, the "Swing" and "Stance" phase of the leg during gait. Firstly, we were able to achieve the desired motion during the whole stride ($RMSE_{knee} = 10.3°$, $RMSE_{ankle} = 1.8°$), and, secondly and more importantly, it was shown that this was done by only one EHA unit with the help of the valves, which is the basis of the under-actuation and the innovative part of this prosthesis. This prosthesis could possibly be advantageous for several reasons: lightweight (4kg conservative estimation) if compared with fully active knee-ankle prostheses (4.5-5 kg) and being able to actuate simultaneously knee and ankle joints.
In addition, partial assistance (with respect to the 100% of force a physiological leg would normally exert) could be given during high torque demanding tasks. This is supported by the possibility of shutting off one valve completely in order to give power only to one joint, which could be useful for tasks such as the stair ascent. Moreover, the under-actuation approach could possibly reduce bulkiness and energy consumption, leading to a higher autonomy of the prosthesis.
As possible future developments, actuation unit plus valves prototyping could be considered to execute preliminary tests. In addition, a better control strategy could be implemented, especially one in closed loop, possibly utilizing more complex techniques such as Reinforcement Learning or non-linear control strategies. Eventually, a prototype of the leg could be built to practically test the results of the work and advance in the research of such type of prosthesis.

Bibliography

[1] *100 years of prosthesis: How war amputees have driven design innovation.* URL: https://www.abc.net.au/news/2016-04-21/how-war-amputees-drove-the-prosthetics-industry/7342626 (cit. on p. 1).

[2] Mark Karadsheh MD. *Gait cycle.* URL: https://www.orthobullets.com/foot-and-ankle/7001/gait-cycle (cit. on p. 3).

[3] *L'amputazione.* URL: http://chirurgiadelmoncone.org (cit. on p. 3).

[4] Michael Windrich, Martin Grimmer, Oliver Christ, Stephan Rinderknecht, and Philipp Beckerle. «Active lower limb prosthetics: a systematic review of design issues and solutions». In: *Biomedical engineering online* 15.3 (2016), pp. 5–19 (cit. on p. 3).

[5] Frank Sup, Amit Bohara, and Michael Goldfarb. «Design and control of a powered transfemoral prosthesis». In: *The International journal of robotics research* 27.2 (2008), pp. 263–273 (cit. on p. 4).

[6] Brian J Hafner, Joan E Sanders, Joseph Czerniecki, and John Fergason. «Energy storage and return prostheses: does patient perception correlate with biomechanical analysis?» In: *Clinical Biomechanics* 17.5 (2002), pp. 325–344 (cit. on p. 5).

[7] Chandrasekaran Jayaraman et al. «Impact of powered knee-ankle prosthesis on low back muscle mechanics in transfemoral amputees: A case series». In: *Frontiers in neuroscience* 12 (2018), p. 134 (cit. on pp. 5, 6).

[8] B. Aeyels, L. Peeraer, J. Vander Sloten, and G. Van der Perre. «Development of an above-knee prosthesis equipped with a microcomputer-controlled knee joint: first test results». In: *Journal of Biomedical Engineering* 14.3 (1992). Annual Scientific Meeting, pp. 199–202. ISSN: 0141-5425. DOI: https://doi.org/10.1016/0141-5425(92)90052-M. URL: https://www.sciencedirect.com/science/article/pii/014154259290052M (cit. on p. 5).

[9] *C-Leg 4 Ottobock.* URL: https://www.ottobock.com/it-it/product/3C88-3~23C98-3 (cit. on pp. 5, 7).

[10] *Power Knee Ossur*. URL: https://www.ossur.com/en-us/prosthetics/knees/power-knee (cit. on p. 6).

[11] Frank Sup, Huseyin Atakan Varol, Jason Mitchell, Thomas J Withrow, and Michael Goldfarb. «Self-contained powered knee and ankle prosthesis: Initial evaluation on a transfemoral amputee». In: *2009 IEEE International Conference on Rehabilitation Robotics*. IEEE. 2009, pp. 638–644 (cit. on p. 6).

[12] Jason Edward Mitchell. «Design of modular self contained knee and ankle prostheses». PhD thesis. 2014 (cit. on p. 6).

[13] *Designing simple hydraulic joints*. URL: http://projecthexapod.com/blog/wp-content/uploads/2012/06/Designing-Simple-Hydraulic-Joints-2012-06-10.pdf (cit. on p. 7).

[14] *Motor*. URL: https://www.epaddock.it/en/the-motor-for-the-motoe/ (cit. on p. 9).

[15] Marco Puliti, Federico Tessari, Renato Galluzzi, Andrea Tonoli, and Nicola Amati. «Design Methodology of Gerotor Hydraulic Machines for Mechatronic Applications». In: *ASME International Mechanical Engineering Congress and Exposition*. Vol. 85604. American Society of Mechanical Engineers. 2021, V006T06A029 (cit. on p. 9).

[16] Massimo Rundo and Nicola Nervegna. «Lubrication pumps for internal combustion engines: a review». In: *International Journal of Fluid Power* 16.2 (2015), pp. 59–74 (cit. on p. 9).

[17] *Gerotor and IGR Technology*. URL: https://www.casconpump.com/gerotors/ (cit. on p. 10).

[18] Federico Tessari, Renato Galluzzi, Andrea Tonoli, Nicola Amati, Giovanni Milandri, Matteo Laffranchi, and Lorenzo De Michieli. «An integrated, backdrivable electro-hydrostatic actuator for a knee prosthesis». In: *2020 8th IEEE RAS/EMBS International Conference for Biomedical Robotics and Biomechatronics (BioRob)*. IEEE. 2020, pp. 708–714 (cit. on pp. 10, 11, 23, 30).

[19] Renato Galluzzi, Yijun Xu, Nicola Amati, and Andrea Tonoli. «Optimized design and characterization of motor-pump unit for energy-regenerative shock absorbers». In: *Applied Energy* 210 (2018), pp. 16–27 (cit. on p. 10).

[20] Federico Tessari, Renato Galluzzi, Andrea Tonoli, Nicola Amati, Matteo Laffranchi, and Lorenzo De Michieli. «Analysis, Development and Evaluation of Electro-Hydrostatic Technology for Lower Limb Prostheses Applications». In: *2020 IEEE/RSJ International Conference on Intelligent Robots and Systems (IROS)*. IEEE. 2020, pp. 3377–3382 (cit. on pp. 10, 11).

[21] Tiziana Lencioni, Ilaria Carpinella, Marco Rabuffetti, Alberto Marzegan, and Maurizio Ferrarin. «Human kinematic, kinetic and EMG data during different walking and stair ascending and descending tasks». In: *Scientific data* 6.1 (2019), pp. 1–10 (cit. on pp. 12, 13, 54, 58).

[22] Alvin R Tilley et al. *The measure of man and woman: human factors in design*. John Wiley & Sons, 2001, p. 12 (cit. on p. 13).

[23] Ge Wu et al. «ISB recommendation on definitions of joint coordinate system of various joints for the reporting of human joint motion—part I: ankle, hip, and spine». In: *Journal of biomechanics* 35.4 (2002), pp. 543–548 (cit. on pp. 13, 14).

[24] Edward S Grood and Wilfredo J Suntay. «A joint coordinate system for the clinical description of three-dimensional motions: application to the knee». In: *Journal of biomechanical engineering* 105.2 (1983), pp. 136–144 (cit. on p. 13).

[25] *Ankle Range of Motion Test*. URL: https://orthofixar.com/special-test/ankle-range-of-motion/ (cit. on p. 15).

[26] *ilm-e70x18*. URL: https://www.tq-group.com/de/produkte/tq-robodrive/servo-kits/ilm-e70x18/ (cit. on p. 28).

[27] Albert Wang and Sangbae Kim. «Directional efficiency in geared transmissions: Characterization of backdrivability towards improved proprioceptive control». In: *2015 IEEE International Conference on Robotics and Automation (ICRA)*. 2015, pp. 1055–1062. DOI: 10.1109/ICRA.2015.7139307 (cit. on p. 28).

[28] Federico Tessari, Renato Galluzzi, and Nicola Amati. «Efficiency-Driven Design Methodology of Gerotor Hydraulic Units». In: *Journal of Mechanical Design* 142.6 (Dec. 2019). 063501. ISSN: 1050-0472. DOI: 10.1115/1.4045421. eprint: https://asmedigitalcollection.asme.org/mechanicaldesign/article-pdf/142/6/063501/6531866/md_142_6_063501.pdf. URL: https://doi.org/10.1115/1.4045421 (cit. on p. 29).

[29] Marco Puliti, Federico Tessari, Renato Galluzzi, Andrea Tonoli, and N. Amati. «Design Methodology of Gerotor Hydraulic Machines for Mechatronic Applications». In: Nov. 2021. DOI: 10.1115/IMECE2021-73205 (cit. on p. 29).

[30] *ilm50x08 datasheet*. URL: https://www.tq-group.com/filedownloads/files/products/robodrive/extended_data-sheets/drva_db-lim-kits_ilm50x08_rev200.pdf (cit. on pp. 30, 34, 42, 43).

[31] David A Winter. *Biomechanics and motor control of human movement*. John Wiley & Sons, 2009 (cit. on pp. 35, 38, 58).

[32] *Multibody Multiphysics library*. URL: https://it.mathworks.com/matlabcentral/fileexchange/37636-simscape-multibody-multiphysics-library (cit. on p. 46).

[33] *simulink-multibody*. URL: https://www.mathworks.com/products/simscape-multibody.html (cit. on p. 50).